Elucidation of the biochemical pathways involved in two distinct cut-surface discolouration phenotypes of lettuce

by Hunter, P.J., Chadwick, M., Graceson, A., Hambidge, A., Hand, P., Heath, J., Lignou, S., Oruna-Concha, M.J., Pink, D., Rada, B., Wagstaff, C., Barker, G. and Monaghan, J.M.

DOI link to the version of record on the publisher's website

Hunter, P.J., Chadwick, M., Graceson, A., Hambidge, A., Hand, P., Heath, J., Lignou, S., Oruna-Concha, M.J., Pink, D., Rada, B., Wagstaff, C., Barker, G. and Monaghan, J.M. (2022) 'Elucidation of the biochemical pathways involved in two distinct cut-surface discolouration phenotypes of lettuce', *Postharvest Biology and Technology*, *183* (111753)

Elucidation of the biochemical pathways involved in two distinct cut-surface discolouration phenotypes of lettuce.

Paul J. Hunter[1], Martin Chadwick[2], Abigail Graceson[1], Angela Hambidge[3], Paul Hand[1], Jennifer Heath[1], Stella Lignou[2], Maria Jose Oruna-Concha[2], David Pink[1], Bindukala Rada[2], Carol Wagstaff[2], Guy Barker[3], James M. Monaghan[1*]

[1] Fresh Produce Research Centre, Harper Adams University, Newport, Shropshire TF10 8NB, UK

*corresponding author

jmmonaghan@harper-adams.ac.uk

[2]Department of Food and Nutritional Sciences, University of Reading, Harry Nursten Building, Pepper Lane, Whiteknights, Reading, RG6 6DZ, UK

[3] School of Life Sciences, University of Warwick, Gibbet Hill Road, Coventry, CV4 7AL, UK

Running Title: Biochemistry of lettuce pinking and browning

Abstract

To understand better the biochemistry and underlying genetic control of postharvest discolouration in lettuce, an F_7 recombinant inbred population (Saladin x Iceberg) was grown in field trials and phenotyped. We identified two distinct discolouration phenotypes, pinking and browning, which were negatively correlated at the phenotypic

level and located six QTL associated with pinking and five QTL associated with browning plus two QTL associated with total discolouration which could not be attributed to either type, on an improved genetic map. Candidate genes underlying QTL were investigated. Plants showing extremes of discolouration were also grown under controlled environment conditions. Lines showing extreme phenotypes from both environments were used for transcriptome profiling and differentially expressed transcripts associated with pinking and browning were identified. Involvement of the phenylpropanoid, flavonoid and terpenoid biosynthesis pathways were indicated in the development of discolouration, with the point of divergence for development of the different discolouration phenotypes localised to the phenylpropanoid pathway. Other biochemistry including amino acid metabolism was also implicated with environmental factors including temperature, water availability and physical stress indicated as potential contributory factors. Differential transcriptional control may be involved in regulating discolouration, potentially through stereochemical selection.

KEYWORDS: Lettuce discoloration, pinking, browning, differentially expressed transcripts, QTL.

1 Introduction

Many leafy vegetables, including lettuce (*Lactuca sativa*), are susceptible to postharvest discolouration. Minimal processing adds value to fresh produce (Soininen, 2009), but also increases perishability, reducing shelf-life and increasing waste. “Pinking” or “browning” discolouration at the cut surface of processed lettuce due to the accumulation of pigmented compounds is believed to occur via action of polyphenol oxidases (PPO) on phenolic compounds from the phenylpropanoid pathway. This leads

to the formation of quinones which then polymerize, or react with amino acids and proteins to form pigments (Zawistowski *et al*., 1991; Martinez and Whitaker, 1995; Solomon *et al.,* 1996; Gawlik-Diziki *et al.,* 2008; Toivonen and Brummell 2008; García et al., 2018; Saltveit 2018; García et al., 2019). In healthy plant tissue PPO and polyphenolic compounds are separated by sub-cellular compartmentalization; PPO in the chloroplast and the majority of polyphenol products in the vacuole (Toivonen and Brummell, 2008). Mechanical damage during processing compromises this compartmentalization at the wound surface, allowing mixing of PPO and phenolic substrates (Kays, 1999; Hilton *et al.*, 2009; Degl'Innocenti *et al.,* 2005; Querioz *et al.*, 2008; Toivonen and Brummell, 2008).

Genetic variation (Atkinson *et al.,* 2013a) and the environment the plant encounters during growth (Lee and Kader, 2000) have both been shown to be major factors in determining postharvest quality and shelf-life of fresh-cut lettuce. Environmental factors associated with discolouration include temperature, nutrient (particularly nitrogen) availability, maturity at harvest, rainfall, temperature, light exposure (particularly UV), and potentially microbial colonization (Hunter *et al.,* 2017). Whilst improved processing techniques (including modified atmosphere packaging) can help reduce post-processing discolouration, an alternative strategy is to manipulate plant biochemistry either at a chemical or genetic level. In order for this to be effective, an in-depth understanding of the biochemical processes and the underlying genetic control of plant pathways involved is required.

In this study, we have used a set of 94 F_7 recombinant inbred lettuce lines (RILs) with previously demonstrated variation in the development of pinking and browning discolouration. The parents of the population were *L. sativa* cv Saladin, an iceberg type and *L. sativa* cv Iceberg, a batavian type (Atkinson *et al*., 2013a). The RILs were grown

in field trials and chopped, bagged and stored in a cooled environment typical of commercial practice. Discolouration was assessed over a 3-day postharvest storage period. Lines selected as showing consistently high and low levels of discolouration were also grown under controlled environment (CE) conditions and transcriptomic analyses of both field-grown and CE material were performed. In addition, quantification of discolouration phenotypes was used to locate QTL on a revised Saladin x Iceberg genetic map and putative candidate genes underlying QTL were identified.

2 Materials and Methods

2.1 Plant production – Field trials

The field studies utilised the 94 most informative lines of a *Lactuca sativa* Saladin x Iceberg RIL population (Atkinson *et al* 2013a) and parents. Field trials were conducted at Harper Adams University, Shropshire in central UK (Grid Ref SJ 711200) over three consecutive years (2015 - 2017). Multiple sowings were grown in each year (Table 1).

Table 1. Growth periods and average environmental conditions for each trial.

Year	Trial	Transplant Date	Harvest Date	Mean Daily Average Air Temperature (ºC)	Mean Daily Rainfall (mm)	Mean Daily Solar Energy (MJ)
2015	1	16 June	25 August	15.6	2.0	16.1
	2	23 June	25 August	15.8	2.2	15.7
	3	30 June	26 August	15.8	2.4	15.0
2016	4	14 April	21 June	11.8	2.0	16.5
	5	10 May	5 July	14.1	2.4	16.8
	(6)	Trial abandoned				
	7	3 August	27 September	16.0	1.7	11.8
2017	8	6 June	31 July	16.2	1.7	16.4
	9	20 June	14 August	16.0	2.3	15.0

Plant production followed commercial practice. Seed were sown 1.5 cm deep in pre-formed 3 x 3 x 4 cm commercial peat plugs with a 0.5 cm diameter hole (provided by G's Fresh, Cambridgeshire, UK). Seeds were covered with vermiculite, watered and maintained at 15 ºC in the dark until emergence. Emerged seedlings were transferred to a mesh sided polytunnel under ambient temperature and light until they reached the 3-4 true leaf growth stage (approximately two weeks). Seedlings were then transplanted into prepared field plots.

Field plots were sub-soiled to a depth of 40 cm, ploughed to a depth of 20 cm and power-harrowed to a depth of 10 cm using a power-harrow fitted with packer-roller. Soil samples were taken for moisture and nutrient analyses and the results used to calculate nutrient input (Defra, 2010). A top-dressing of an additional 50 kg ha^{-1} N was applied 2 weeks post-transplanting. In addition, pre-emergence herbicides Stomp-Aqua (BASF) and Wing-P (BASF) were applied at 1 L ha^{-1} and 1.25 L ha^{-1} respectively in the 2015 and 2016 trials.

Seedlings were transplanted into randomized trials in blocks of 12 plants per line in a 3x4 grid in 2015 and 2016 and blocks of 6 plants per line in a 2 x 3 grid in 2017. Spacing was 40 cm between planting stations in 2015 and 60 cm between stations in 2016 and 2017. Trials were irrigated with overhead spray in 2015 and drip tape in 2016 and 2017 to maintain commercially recommended soil moisture levels (ADAS, 2007).

Metaldehyde slug pellets were applied at transplanting and re-applied as necessary. Fungicide protection was achieved with 2 kg ha^{-1} Karamate (Indofil Industries B.V., Amsterdam, Netherlands.) with 0.8 kg ha^{-1} Switch (Syngenta UK Ltd, Fulbourn, UK) at 7 days post-transplanting, 2 kg ha^{-1} Invader (BASF (UK), Littlehampton UK) with 1.5 kg ha^{-1} Signum (BASF) at 17 days post-transplanting, 1.9 kg ha^{-1} Fubol Gold (Syngenta) with 0.5 L ha^{-1} Movento (Bayer AG, Monheim am Rhein, Germany) at 27 days post-transplanting (with the additional inclusion of 0.075 L ha^{-1} Hallmark (Syngenta) if disease pressure was considered high), and 0.6 L ha^{-1} Revus (Syngenta) with 250 mL ha^{-1} Decis (Bayer) at 37 days post-transplanting.

2.2 Plant production – CE

Lines exhibiting consistently high or low pinking or browning responses were identified based on the 2015 and 2016 field trials and previous work (Atkinson *et al.,* 2013a) and plants of these lines were also grown in controlled environment (CE) over winter in 2016 (Table 2). Seeds were sown into Levington F2S compost (Scotts Professional, Ipswich, UK) in 5 x 8 cell modular trays (Plant Pak P40, Desch Plantpak Ltd, Maldon, UK) and kept in the dark at 15 ºC until emergence. Three replicate seedlings of each were then potted on into 1 L pots of M2 compost (Levington) amended with 2 g L^{-1} Osmocote (ICL group, Tel Aviv, Israel) slow release NPK

fertiliser. Seedlings were randomly arranged in a CE cabinet (Weiss Technik UK Ltd, Loughborough, UK) and maintained under a 16 hour day / 8 hour night light cycle, 18 ºC /15 ºC (day / night) temperature, 90 % relative humidity and ambient CO_2.

139

Table 2. Lines exhibiting consistently high or consistently low pinking or browning responses used for RNA extraction.

Plants Grown in CE (2016)

		Average Pinking Index Value		
Line	**Phenotype**	**2015**	**2016**	**2017**
10045	**HP**	166.7	93.9	106.9
10055	**HP**	236.1	155.5	152.8
10095	**HP**	175.5	63.3	175.0
10023	**LP**	31.5	19.3	8.3
10043	**LP**	26.9	3.8	17.5
10073[a]	**LP**	10.2	3.8	13.4

		Average Browning Index Values		
Line	**Phenotype**	**2015**	**2016**	**2017**
10022[b]	**HB**	189.8	95.7	128.1
10053[c]	**HB**	106.5	39.6	168.8
10069	**HB**	149.1	27.3	124.3
10043	**LB**	57.4	44.0	64.1
10045	**LB**	79.6	25.2	113.4
10051	**LB**	59.3	13.0	50.2

Additional Field Grown Lines (2016)

		Average Pinking Index Value		
Line	**Phenotype**	**2015**	**2016**	**2017**
10088[d]	**LP**	67.1	15.8	83.5

		Average Browning Index Values		
Line	**Phenotype**	**2015**	**2016**	**2017**
10029[e]	**HB**	117.8	91.7	128.3
10030[f]	**HB**	141.9	43.1	110.4

140 HP: lines showing consistently high levels of pinking, LP: lines showing consistently low levels of
141 pinking, HB: lines showing consistently high levels of browning, LB: lines showing consistently low
142 levels of browning. [a,b,c]: lines not available for RNASeq analysis from field material due to poor quality
143 RNA, [d,e,f]: the replacement field lines used for transcriptome analysis. CE conditions; 16-18°C daytime
144 temperature, 10-12°C night-time temperature, 16 hour day / 8 hour night light cycle with broad spectrum
145 illumination, 85% relative humidity.

146 2.3 Harvest and processing

147 In the field trials, the central two heads in each block were harvested when more than
148 half of the lines had reached market maturity, the remaining heads acted as guard plants.
149 The two heads were treated as separate samples. Heads were cut in the morning and
150 transferred to 5 ºC to remove field heat. The outer (wrapper) leaves were removed
151 before heads were quartered longitudinally, the core removed and leaf material cut into
152 approximately 3 x 3 cm pieces. Cut material was mixed and approximately 100 g of
153 material transferred to each of three commercial microperforated pillow pack bags
154 (Amcor 35PA240; Amcor Flexibles, Bristol, UK). Bags were heat sealed, the seals were
155 checked visually for integrity and the bags were placed into cold storage at 5 ºC in the
156 dark. Replicate bags were removed from cold storage after approximately 2 hours (0
157 days postharvest), 1 day and 3 days and discolouration recorded. Recorded samples
158 were then transferred to -80 ºC for long term storage. In the CE trials, plants were
159 harvested at 8 weeks post-transplanting, processed, stored and recorded in the same
160 manner as the field grown material.

161

162 2.4 Scoring of discolouration

163 Pillow packs were overlaid with a 3 x 4 grid composed of 12, 6 x 6 cm squares. Pinking
164 and browning symptoms were manually scored separately in each square on a 5-point
165 system with reference to photographic standards reported in Hilton *et al*. (2009), as
166 used by Atkinson *et al.* (2013a); 0 – no appearance of discolouration, 1 – slight
167 discolouration but unable to differentiate between pinking or browning (a score of 1 for
168 both symptoms), 2 - low level discolouration (scored separately for pinking and
169 browning), 3 - intermediate discolouration (scored separately for pinking and
170 browning), 4 severe discolouration (scored separately for pinking and browning). An

171 average score for each symptom for each bag (symptom intensity) was recorded across
172 the 12 grids, including scores 0 to 4. The percentage for grid squares with intensity
173 scores between 1 and 4 were also recorded (symptom incidence) and a symptom index
174 calculated as a product of the intensity and incidence.
175
176 2.5 Mapping and QTL analysis
177 In order to improve the marker density of the previously published Saladin x Iceberg
178 linkage map (Atkinson *et al.,* 2013b), additional KASP markers were derived from
179 single nucleotide polymorphisms (SNPs) between the genomic sequences of the
180 parents. For SNP identification total RNA extracts were made from each parental line
181 and mRNA selected using oligo(dT) Dynal magnetic beads (Invitrogen, MA, USA)).
182 The integrity of RNA was confirmed on a Bioanalyser (Agilent Technologies LDA UK
183 Ltd, Stockport, UK). TruSeq (Illumina Inc., San Diego, CA, USA) libraries prepared
184 from this material were sequenced on a HiSEQ (Illumina) platform to produce 70nt
185 single end reads.
186 A lettuce reference sequence database was constructed comprising candidate
187 genes for the phenylpropanoid pathway, leaf senescence, nitrate use efficiency,
188 flowering time, and ESTs from the CLS_S3_Sat.assembly (L. sativa|CAP3:100/95)
189 database (http://cgpdb.ucdavis.edu/cgpdb2/est_info_assembly.php). Reads were base-
190 called and scored for read quality and aligned to the reference EST sequences using
191 Bowtie v0.11.3 (Langmead *et al*., 2009), and consensus sequences generated for each
192 accession using SAMtools (Li *et al*., 2009). SNP loci were then identified between
193 consensus sequences using a custom Perl pipeline. Loci with very low coverage or
194 sequencing quality (Phred score < 33) in either accession were discounted. Unique
195 SNPs amenable to unambiguous PCR were identified by aligning 150 nt regions of the

196 consensus sequence around each SNP to the reference database using BLAST (Altschul
197 *et al.,* 1990) at > 98 % identity. This resulted in 1395 SNPs from which 682 unique
198 KASP markers were developed. 78 potential markers were eliminated in quality checks
199 resulting in 604 additional KASP markers. Combined with the data from the previous
200 version of the map, the extended lettuce mapping dataset contained 1028 loci scored
201 over 108 individuals from the Saladin x Iceberg F_7 population. A linkage map was
202 constructed using the Kosambi mapping function (LOD threshold 0.01, recombination
203 frequency threshold 0.49, jump threshold 5.0, ripple value 1) in Joinmap 4.0 (Van
204 Ooijen, 2018). Loci were grouped using Independence LOD and mapping groups were
205 selected at LOD 5-6. Loci with high recombination frequency and LOD score or with
206 SCL values > 5.0 were excluded.
207 Each 100bp region containing a SNP was aligned to a pseudo-chromosome
208 genomic locus from a draft *L. sativa* genome assembly 'Lsat_1_v4', accessed from the
209 U.C. Davis lettuce genome resource site (http://lgr.genomecenter.ucdavis.edu). The
210 assembly comprises 1.5 Gb of sequence as 9 pseudo-chromosomes. Unmapped SNPs
211 were included as an additional group. The final map contained 27 groups aligned with
212 lettuce pseudo-chromosomes using KASP markers. 2 groups could not be aligned with
213 lettuce pseudo-chromosomes due to lack of corresponding markers.
214 For QTL analyses, discolouration severity and index values were
215 logarithmically transformed according to the formula $v = \ln (x + 2)$ and discolouration
216 incidence and qRT-PCR expression values (%) were ArcSine transformed prior to
217 analysis. QTL analysis was conducted using MapQTL v6 (Van Ooijen, 2009). Initial
218 QTL were positioned using a combination of Kruskal-Wallace and Interval Mapping
219 using data across all available trials. Initial QTL locations were used as cofactors for
220 subsequent multiple QTL model (MQM) analyses. MQM analyses were conducted

iteratively with each round of QTL locations being used as cofactors in the subsequent round until no further movement in QTL positions occurred. In all cases the head morphotype was included as a co-variant to exclude morphology effects. Significant QTL were identified based on LOD scores above the genome wide LOD threshold calculated according to the Permutation Test protocol of the software. Genes underlying QTL with at least a one base overlap of the QTL region were identified using Bedtools (Quinlan and Hall, 2010), with gene locations determined from the U.C. Davis Lettuce Genome Resource (http://lgr.genomecenter.ucdavis.edu/). Six-frame translations of the genes were generated using the EMBOSS tranSeq tool (Maderira *et al.,* 2019). Annotation was added by comparing these translations against the NCBI RefSeq Non-Redundant proteins database (Pruitt *et al.,* 2005), using DIAMOND (Buchfink *et al.,* 2015) in the 'more-sensitive' mode with an e-value cut-off of 0.001. Predicted function and family membership was determined by searching for functional regions in the translations using InterProScan (Jones *et al.,* 2014).

2.6 RNA extraction and transcription profiling

Frozen plant material from trials 5 and 7, and from CE plants, was freeze-dried and milled to a homogeneous powder. 50-60 mg was extracted using the FastRNA Green protocol (MP Biomedical, Santa Ana, CA, USA), with a 40 s homogenization at setting 6.0 on the FastPrep homogenizer and the inclusion of a second chloroform extraction. Extracted RNA was re-suspended in 100 µL of DEPC-treated water and further purified using the RNeasy Mini RNA clean up protocol (Qiagen UK Ltd, Manchester, UK) with elution in 60 µL of sterile nuclease-free water (Invitrogen). RNA concentration was determined using a Qubit fluorometer (Invitrogen) with the

RNA high sensitivity (HS) buffer system. Quantified RNA was stored at -80 ºC for further use.

For transcription profiling, TruSeq RNA (Illumina) libraries were prepared from RNA of field grown plants representing the identified consistently high and low discolouring lines (Table 2) in trials 5 and 7. Additional libraries were prepared from RNA of these lines grown under CE conditions (12 lines x 3 time points). Libraries were sequenced as for the mapping (above) with the exception that 150 bp single end reads were generated to an approximate depth of 30 million reads per library.

Reads were quality checked using Fastqc (Andrews, 2010) and MultiQC (Ewels *et al.,* 2016). Adapters and poor-quality sequence ("quality 20") were removed using CutAdapt (Martin, 2011). PhiX control sequences were removed using BBduk (Bushnell) with arguments "k=31" and "hdist=1". Reads were aligned to the lettuce genome using STAR (Dobin *et al.,* 2013) with a "sjdbOverhang" parameter of 149. The lettuce genome (ID 35223) was downloaded from CoGe (Lyons and Freeling, 2008) and annotated with similarity, protein function and orthology using DIAMOND (Buchfink *et al.,* 2015) and InterProScan (Jones *et al.,* 2014) as above and with EggNOG-mapper (Huerta-Cepas *et al.,* 2017) using the eukaryote database "euNOG" with 1:1 orthologs and "Experimental Only" Gene Ontology evidence. Uniquely mapped reads were counted using FeatureCounts (Liao *et al.,* 2014) with argument "-s 2" and analysed in DESeq2 (Love *et al.,* 2014) with default settings, in R v 3.2.3 (R core team, 2018). Trials 5, 7 and the CE samples were analysed separately. Differential expression was tested between pooled data representing high and low pinking and browning, and also between samples representing high and low expression of pinking and browning. Functional enrichment of Gene Ontology, KEGG Orthology and Cluster of Orthologous Groups terms from EggNOG-mapper gene annotations was determined

using the goseq package (Young *et al.,* 2010). For this enrichment analysis, a significance cut-off of Benjamini-Hochberg adjusted P value < 0.1 was used to determine the differentially expressed genes. A maximum P value of 0.1 was also used for significant enrichment of function terms. Following analysis, transcripts were selected which showed 3-fold or greater expression level differences consistently across the two field trials or the three CE replicates. Transcripts which did not generate a predicted protein sequence or a sequence that could not be identified by homology were excluded.

2.7 qRT-PCR

Primers were designed for target transcripts from sequences located on the lettuce genome sequence assembly 'Lsat_1_v8', (http://lgr.genomecenter.ucdavis.edu). Gene and cDNA sequences were aligned to identify intron regions. Primers for 100-200 bp amplicons were designed with one primer extending across an intron excision site where possible, to ensure no unintentional amplification signal from contaminating genomic DNA (Table S1). Primers were tested on RNA extracts from the parent plants of the cross, the optimum annealing temperatures determined and the resulting amplicons sequenced to confirm target identity.

Table S1. Primer sequences and associated melting temperatures (Tm) and reaction annealing temperatures (Tann) used for qRT-PCR studies.

Target	Forward primer sequence	Tm (oC)	Reverse primer sequence	Tm (oC)	Tann (oC)
Absicic acid hydrolase 4	atgccaattacgtacaaggtgatat*	59	aacttcccagcttaacaactccta	61	56
Chalcone synthase	gcgcatgtgtgacaagtctatg*	63	aagaaatggctcgaacccctgaag	64	58
Phenylaniline ammonia lyase	agttaaggcgagtagtgattgggtt*	63	tttagattactcgaggaagaca	57	52
Polyphenol oxidase[a]	cacaaatattctcgacttcaaacca		ctcggtagcgttatgcgtgtt		
Trans-cinnamate 4-monooxygenase	catcaacgttgctgcaatcgaaaca*	63	tgccagacctccatcccctcaaaac	68	58
Chalcone-flavonone isomerase	aggtatctgaaatgtgcgttggtg	63	agctcttcgactaactttcactt*	59	54
Flavonoid-3'-monooxygenase	cgctagcagaccaccgaactcc	68	cgatggaggaggacggcttgc*	68	63
NAD(P)H-quinone oxidoreductase	ttcttggcaggaacgagttatgata	61	ttcttttaagacgttgttttggtga*	58	53
Reference sequences					
Actin12[a]	acctcagcagaacgtgaaattgtaa	61	gagcattgagaagagttgtctgctt	63	56
Protein phosphatase 2A regulatory subunit A3	catgcaatggttacaagacaaggtat*	61	gtttgaggaggcgttcagagaag	64	56
TIP41	tttgtatggagatgaattggctgata	61	ccatcaactctaagccagaaacgt*	63	56

*primers designed across exon / intron boundaries, [a] gene sequence did not contain intron regions

For qRT-PCR, 250 ng of RNA from each field sample from trials 5 and 7 was first denatured for 5 min at 65 ºC in the presence of 250 ng oligo(dT)$_{12-18}$ reverse primer (Invitrogen). First strand cDNA synthesis for 50 min at 42 ºC, followed by incubation for 15 min at 72 ºC in the presence of 1 mM (each) dNTPs, 12 mM dithiothreitol, 100 units of Superscript II reverse transcriptase (Invitrogen) and 20 units of RNAse OUT RNAse inhibitor (Invitrogen) followed by cooling to 4 ºC. In addition, multiple cDNA samples from parental material were combined for use in preparing a standard curve for quantitation. Standards of 10^0 x – 10^{-4} x relative concentrations of this material were produced by 10-fold serial dilution. Triplicate samples of 1 µL of each cDNA amplification and standard curve dilution and a blank of 5 µL of sterile nuclease free water were combined with 5 µL 2x SensiFast Sybr No-ROX reagent (Bioline Reagents Ltd. London UK), and 1 µL each of 3 µM target specific forward and reverse primer in a LightCycler 480 multiwell 384 well plate (F. Hoffman-La Roche (UK) Ltd, Welwyn Garden City, UK) sealed with a ThermalSeal RT sealing film (Excel Scientific Inc. Victorville CA, USA) qRT-PCR was performed in a LightCycler 480 (Roche) as follows; 3 min denaturation at 95 ºC followed by 45 amplification cycles of 5 s at 95 ºC, 10 s at the appropriate annealing temperature for the primer pairs (Table S1) and 10 s extension at 72 ºC with a single fluorescence acquisition. Following amplification, the melting temperature of the amplicon was determined by denaturing for 5 s at 95 ºC, re-associating the product for 1 min at 65 ºC then increasing temperature at 0.11 ºC s^{-1} to 97 ºC with 5 fluorescence acquisitions per second. Amplification was quantified against the relative standard curve using the Absolute quantification, 2nd derivative maximum method and the *Tm*-calling protocol was used to determine amplicon melting temperatures for all wells.

316 Results which did not fit the melting temperature profile for the appropriate
317 amplicon were discarded. Any signal detected in the averaged blank wells was
318 subtracted from the signal in the sample wells before further data processing. Mean
319 signal values were calculated for each triplicate sample. Expression of actin 12, actin
320 2, alpha tubulin 3, protein phosphatase 2A regulatory subunit A3 (PP2AA3) and TIP41
321 (41kDa TAP42 interacting protein) (Sgamma *et al.,* 2016) were compared for use as
322 internal references. Actin 12, PP2AA3 and TIP41 showed the lowest variation in
323 transcript levels across the RILs and were selected as controls. Values from replicate
324 samples were compared for each of these referents and showed no significant variation
325 between RILs, furthermore ANOVA between the 50 % of samples representing the
326 highest and lowest averaged discolouration indices (for both pinking and browning
327 separately) also showed no significant differences in reference gene expression
328 indicating suitability for use as a normalization standard. All subsequent data was
329 normalized against a geometric mean of the arithmetic mean data from these transcripts.
330

331 ## 3 Results and Discussion

332 There are a number of limitations to the approach described in this paper that should be
333 considered: 1) Discolouration was studied utilising commercially relevant film
334 packaging where respiration rate will have adjusted the pack gas composition during
335 cold storage. This study assumes that there was not a significant variation in respiration
336 rate between RILs. 2) The scoring system relied on a subjective visual assessment of
337 both pinking and browning, using photographic standards. Other workers have
338 reported objective image analysis techniques (e.g. Peng et al., 2021) but these
339 approaches do not yet discriminate between browning and pinking.
340

341 3.1 Discolouration Phenotype

342 Mean discolouration intensity scores, percentage incidence and severity indices for
343 both pinking and browning were calculated from data from all eight field trials. Average
344 index values showed considerable transgressive segregation in the RILs compared to
345 the parent lines (Figure 1).

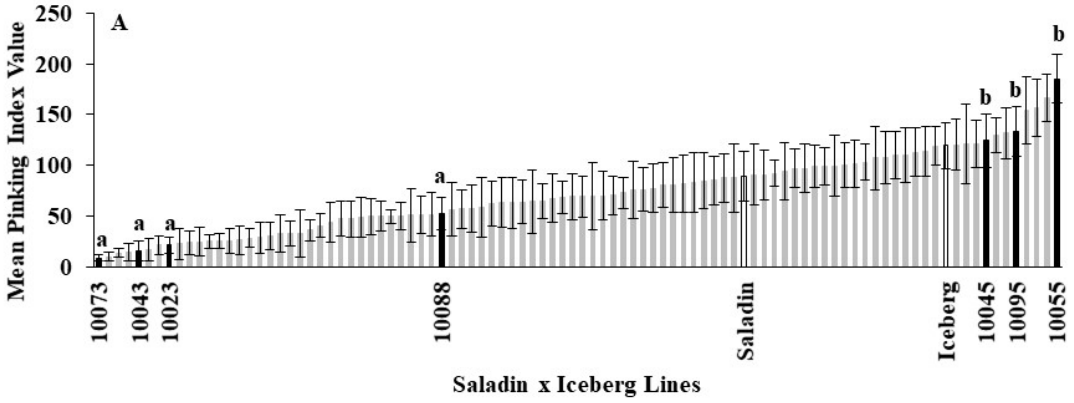

346

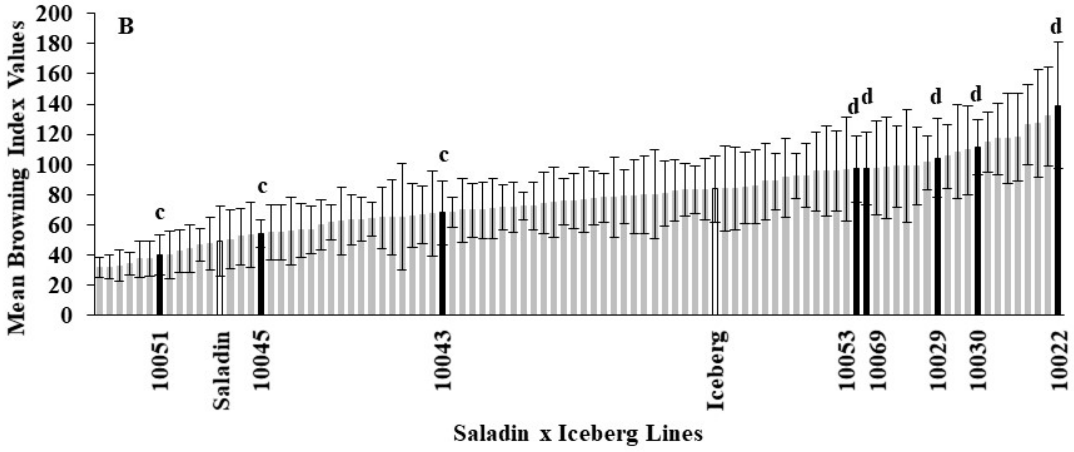

348

(c) and high pinking (b) and browning (d) lines. Error bars show standard error of the mean values.

Data for intensity scores and percentage incidence followed a similar pattern to the index score (Table S2). The browning and pinking index response of the RIL populations were consistent across the 8 experiments (Table S3). The fact that this transgressive segregation can be observed in data averaged from eight separate trials suggests a strong genetic component as well as an environmental response.

Table S2. Pearson correlation of intensity score and percentage incidence with index score for both pinking and browning from each of the 8 trials.

	Pinking		**Browning**	
Trial	**Intensity r value**	**Incidence r value**	**Intensity r value**	**Incidence r value**
1	0.981	0.950	0.969	0.915
2	0.964	0.922	0.978	0.903
3	0.984	0.921	0.985	0.932
4	0.963	0.919	0.932	0.927
5	0.975	0.909	0.956	0.909
7	0.965	0.914	0.954	0.921
8	0.976	0.932	0.976	0.915
9	0.973	0.948	0.982	0.941

Table S3. Pearson correlation of A) Pinking index and B) Browning index across the 8 field trials

A)

Trial	**2**	**3**	**4**	**5**	**7**	**8**	**9**
1	*0.285*	*0.301*	**0.353**	*0.308*	**0.397**	**0.351**	*0.307*
2		0.221	*0.254*	**0.341**	*0.291*	*0.286*	*0.236*
3			**0.468**	**0.428**	**0.499**	**0.417**	*0.300*
4				**0.385**	**0.458**	*0.282*	**0.315**
5					**0.429**	**0.361**	**0.315**
7						*0.263*	*0.248*
8							*0.252*

B)

Trial	**2**	**3**	**4**	**5**	**7**	**8**	**9**
1	**0.722**	**0.735**	**0.744**	**0.733**	**0.697**	**0.711**	**0.714**
2		**0.737**	**0.688**	**0.717**	**0.639**	**0.739**	**0.652**

3	**0.729**	**0.729**	**0.719**	**0.691**	**0.601**
4		**0.746**	**0.705**	**0.738**	**0.728**
5			**0.769**	**0.753**	**0.634**
7				**0.752**	**0.651**
8					**0.788**

Values in plain typeface are significant at P<0.05, those in *italics* are significant at P<0.01 and those in **bold** face are significant at P<0.001

There was a significant dichotomy in mature head morphology noted in the RILs with 49 % having a compact head type similar to Iceberg lettuce, whilst 51 % had a looser head type similar to a Cos variety, however no statistically significant difference in the intensity or incidence of pinking or browning was detected between the two morphotypes. Examination of the relationship between pinking and browning discolouration revealed a significant negative correlation ($p<0.001$) between the two types of discolouration (Figure 2). Data for percentage incidence and severity index show similar significant trends (data not shown). Data from longer term studies conducted over 6 days in trials 1-3 (not shown), suggests that whilst pinking and browning became more intense and more widespread over time, the relative proportion of the different types of discolouration symptoms did not change significantly as would be expected if discolouration were progressing from one state to another, indicating that the two types of discolouration result from separate, but related, processes.

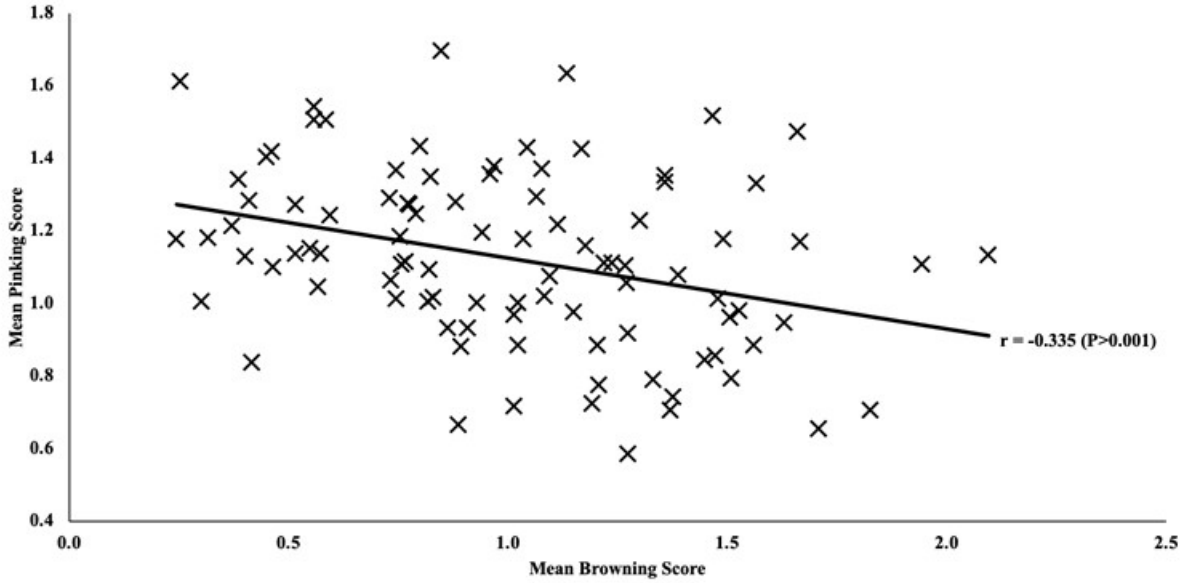

Figure 2.

Scatter plot indicating a negative correlation between pinking and browning discolouration intensity. The intensity scores are averaged for each of the 94 RIL accession across all trials. The trendline indicates a Pearson's correlation coefficient (r) of -0.335 corresponding to a significant negative correlation at $p < 0.001$.

3.2 QTL mapping

QTL mapping of the discolouration phenotypes identified six QTL for pinking (accounting for 17%, 12%, 13%, 8%, 4% and 14% of the observed variation, respectively) and five QTL for browning (accounting for 11%, 13%, 12%, 12%, and 25%). Two additional QTL for overall discolouration (accounting for 33% & 35% of variation) were also identified (Figure 3). The identification of separate QTL for pinking and browning supports the suggestion that the two types of discolouration are biochemically different. A QTL study of processed lettuce decay in modified atmosphere packaging conditions (Hayes *et al*., 2014) identified three QTL for decay with the most significant located on linkage group (LG) 4 and minor QTL on LG 1 and

9a. We identified no QTL on LG 4 of the Saladin x Iceberg map however, and those that did locate to LG 1 and LG 9 were not in the same positions, with the decay QTL identified by Hayes *et al.,* locating to the middle of LG 1 and the very top end of LG 9a. Hayes *et al.* (2014) used a map derived from a slightly different cross, Salinas 88 (derived by backcrossing lettuce mosaic virus resistance into Salinas which is synonymous with Saladin) x La Brilliante. Whilst QTL positions are therefore not directly comparable, the disparity between the QTL locations, especially the lack of a QTL on LG 4 corresponding to the major decay QTL reported by Hayes *et al.* (2014), suggest that it is unlikely that the QTL identified in the current study represent anaerobic decay.

419 Figure 3

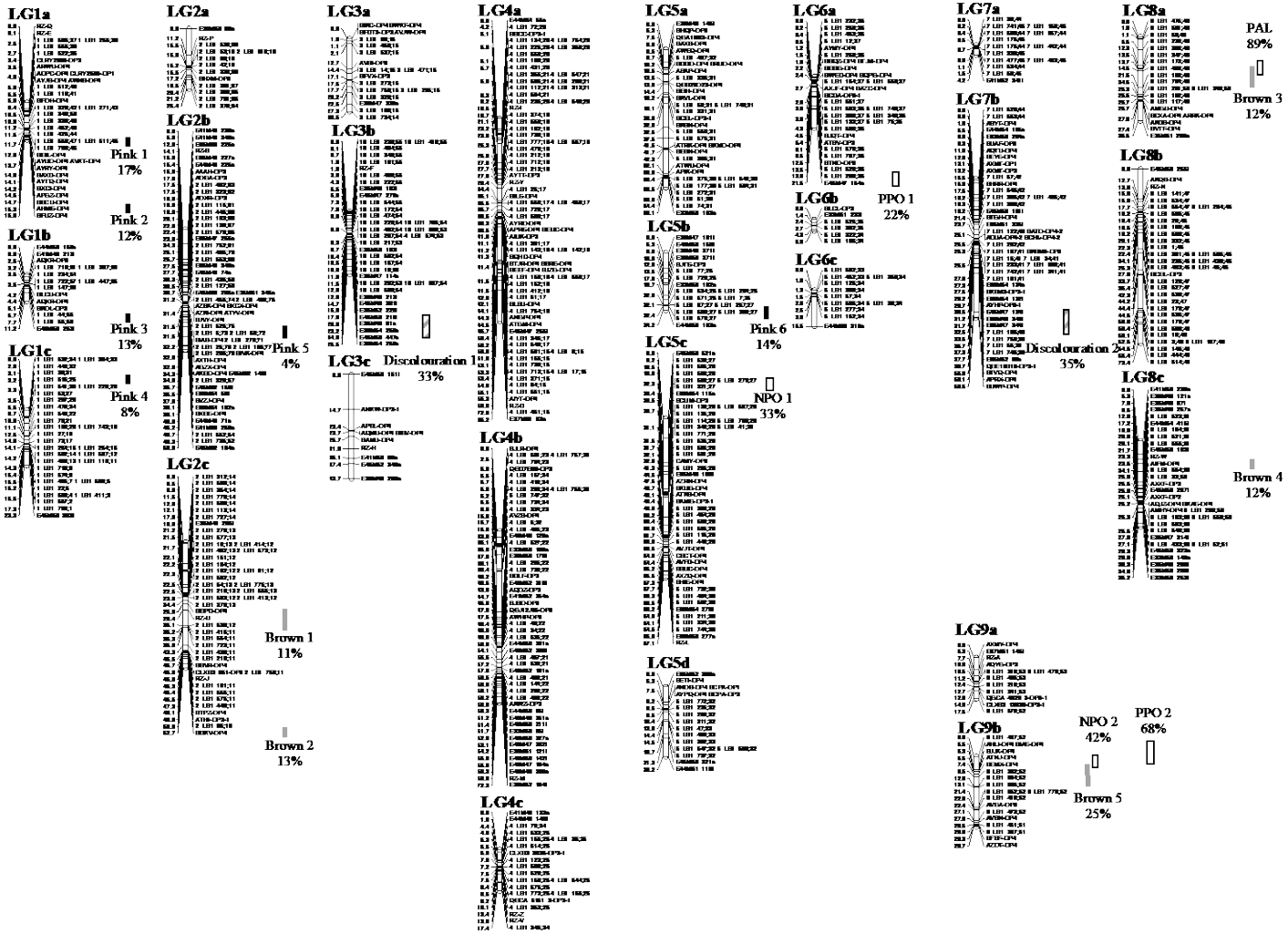
LG1a
LG1b
LG1c
LG2a
LG2b
LG2c
LG3a
LG3b
LG3c
LG4a
LG4b
LG4c
LG5a
LG5b
LG5c
LG5d
LG6a
LG6b
LG6c
LG7a
LG7b
LG8a
LG8b
LG8c
LG9a
LG9b
Pink 1
17%
Pink 2
12%
Pink 3
13%
Pink 4
8%
Pink 5
4%
Pink 6
14%
Brown 1
11%
Brown 2
13%
Brown 3
12%
Brown 4
12%
Brown 5
25%
Discolouration
33%
Discolouration 2
35%
NPO 1
33%
NPO 2
42%
PPO 1
22%
PPO 2
68%
PAL
89%

Figure 3. Revised linkage map of *L. sativa* Saladin x Iceberg. The map consists of 26 linkage groups organized into pseudochromosomes. Mapping produced one additional linkage group of unassociated markers and a number of un-linked markers (not shown as no QTL located to these groups) QTL are identified by vertical bars. Solid black bars indicate QTL associated with pinking (Pink 1-6), grey bars indicate QTL associated with browning (Brown 1-5), hatched bars indicate QTL associated with overall discolouration (Discolouration 1-2) not attributable to either pinking or browning. These QTL are produced from data from all eight field trials. White bars indicate the positions of QTL mapped from data from trials 5 and 7 for the qRT-PCR targets which showed potential co-location with discolouration QTL (PAL = phenylalanine ammonia lyase, PPO = polyphenol oxidase, NPO = NADP-dependent quinone oxidoreductase). Percentage values in the QTL legends indicate the proportion of the observed variation accounted for by the QTL.

Lines selected for consistently high or low levels of pinking and browning were grown in CE trials. Plants in CE had lower pinking and browning indices compared to those seen in field grown plants. Despite the fact that the lines responded consistently across field trials exposed to different environments, the reduced discolouration seen in CE suggests that environmental response may be a factor in the development of both pinking and browning. CE provided control of temperature, moisture availability, humidity and light availability (see Table 2). The spectrum of daylight, is likely to be different in wavelength profile and intensity to that produced in CE. Cultivar-level variation in abundance of some phenolic compounds in response to exposure to different wavelengths of light has previously been observed (Ouzounis *et al.,* 2015; Koukounaras *et al.,* 2016) and UV light exposure has been shown to influence discolouration specifically (reviewed in Hunter *et al.,* 2017). Consequently, a larger pool of phenolic compounds may have been available as substrates for discolouration reactions in field-grown material compared to CE-grown plants. Despite the overall reduction in discolouration in CE-grown material [3-fold browning index, 24-fold pinking index], the selected lines grouped into the same high and low pinking and browning categories as identified in the field trials (Table S4).

Table S4 Spearman rank correlation of pinking and browning intensity score, percentage distribution and index between the 10 selected lines used in the CE and field trials 5 and 7 (2015).

Trial 5	**Incidence r value**	**Distribution r value**	**Index r value**
Pinking	0.714	0.771	0.829
Browning	***0.886***	0.771	(0.638)
Trial 7			
Pinking	0.812	0.771	0.771
Browning	0.725	0.771	***0.886***

Values in plain typeface are significant at P<0.05, those in *italics* are significant at P<0.01 and those in parentheses are not significant at P 0.05.

459

460 3.3 Transcriptome analysis

461 Transcripts showing 3-fold or greater differential expression between samples
462 expressing high and low levels of pinking or browning are indicated in Table S5, whilst
463 those transcripts located between flanking markers for the identified QTL
464 corresponding to pinking, browning or general discolouration are extracted in Table 3.

Table S5. Predicted proteins of transcripts up or down regulated in association with pinking or browning discolouration in mature field grown heads and 8 week post-planting material grown in controlled environment indicating fold increase (+) or decrease (-) in expression relative to non-discoloured material, predicted pathways and association with mapped discoloration QTL.

	Phenotype						
	Field		CE		Co-locating		
Predicted protein	**P**	**B**	**P**	**B**	**QTL**	**UniProt ID**	**Pathway or function**
2-hydroxyphytanoyl-CoA lyase			**+4**			Q54DA9	fatty acid metabolism
3-ketoacyl-CoA synthase			**+3**			Q9SIX1	fatty acid metabolism
3-ketoacyl-CoA synthase 6-like protein	**-3**				D1	A0A2J6LVF7	fatty acid metabolism
3-ketoacyl-CoA synthase 5-like protein		**+4**			B2	A0A2J6LY96	fatty acid metabolism
3-oxo-5-α-steroid 4-dehydrogenase	**-29**				B5	PLY89462	fatty acid metabolism
3-oxoacyl-[ACP] synthase	**-10**	**-6**			B2	A0A2J6JNU8	fatty acid metabolism
α-dioxygenase 1			**-3**		B1	Q9SGH6	fatty acid metabolism
β-ketoacyl synthase	**-8**					PLY86066	fatty acid metabolism
Acyl-ACP thioesterase		**+6**				PLY61749	fatty acid metabolism
Acyl-CoA desaturase	**-5**					A0A2J6MGF8	fatty acid metabolism
Acyl-CoA 5-desaturase AL21			**+3**		P2	P0DOW3	fatty acid metabolism
Acylhydrolase	**+11**	**+12**			D2	PLY91815	fatty acid metabolism
Acyltransferase	**+5**	**-11**			B2	A0A2J6KS02	fatty acid metabolism
Acyl transferase		**+4**			D2	A0A2J6K2S6	fatty acid metabolism
Class 3 Lipase		**-5**				PLY97470	fatty acid metabolism
COBRA-like lipoprotein synthetase		**+6**				A0A2J6LPG0	fatty acid metabolism
Enoyl-(ACP) reductase	**+7**	**-4**			B1	PLY97084	fatty acid metabolism

Enoyl-CoA reductase			**+5**			Q9M2U2	fatty acid metabolism
Epoxide hydrolase	**+4**					A0A2J6MEQ5	fatty acid metabolism
Ethanolamine-phosphate cytidylyltransferase	**+3**				P6	Q9ZVI9	fatty acid metabolism
Fatty acyl-CoA reductase		**+15**			B1	A0A2J6JP17	fatty acid metabolism
Fatty acid synthesis O_2 transporter			**-3**			O24521	fatty acid metabolism
Glutathione S-transferase		**+3**			B4	P32110	fatty acid metabolism
Glycerol phosphate acyltransferase			**+3**			Q9CAY3	fatty acid metabolism
Lecithin:cholesterol acyltransferase		**+4**			B1	A0A2J6MH62	fatty acid metabolism
Lipid transfer protein	**+12**	**+16**	**+5**		D2	PLY95206	fatty acid metabolism
Palmitoyl-monogalactosyldiacylglycerol δ-7 desaturase			**+3**	**+3**	P2	Q949X0	fatty acid metabolism
Phosphatidic acid phosphatase		**-3**				PLY62165	fatty acid metabolism
Omega-3 fatty acid desaturase			**+3**		B4	P48620	fatty acid metabolism
Tensin phosphatase		**-11**			D2	PLY74890	fatty acid metabolism
Very-long-chain enoyl-CoA reductase				**+4**	B2	Q9M2U2	fatty acid metabolism
Alkane hydroxylase MAH1-like			**-5**		B3	A0A2J6JZ74	wax biosynthesis
α-mannosidase		**+3**			B1	Q9LFR0	sugar metabolism
α-mannosyltransferase		**+17**			B5	A0A2J6LGJ2	sugar metabolism
β-galactosidase	**-3**				B4	Q9C6W4	sugar metabolism
Alginate lyase	**+8**	**+8**				PLY89994	sugar metabolism
Exostosin		**+11**			B2	PLY73645	sugar metabolism
Glucan endo-1,3-β-D-glucosidase	**-4**				B3	Q94G86	sugar metabolism
Glucose/ribitol dehydrogenase	**-6**	**-5**			P5	PLY77463	sugar metabolism
Glycoside hydrolase family 2, 9, 17, 47		**-5**				PLY84636	sugar metabolism

Glycosyl hydrolase family 1		**+19**			B5	PLY77220	sugar metabolism
Glycosyl hydrolase family 10	**+16**	**+8**				PLY76647	sugar metabolism
Glycosyl transferase family 8		**+3**			B1	A0A2J6JG41	sugar metabolism
Glycosyl transferase 61		**-4**				PLY67859	sugar metabolism
Invertase	**+16**					PLY86527	sugar metabolism
NAD dependent epimerase		**-11**			B1	A0A2J6KB13	sugar metabolism
Pectate lyase	**-5**		**-3**		D2	PLY64620	sugar metabolism
Phosphoenolpyruvate carboxylase kinase			**+3**			Q9SPK4	sugar metabolism
Phosphoglucose isomerase	**-4**					PLY72051	sugar metabolism
Sucrose synthase	**+5**		**+4**			P49039	sugar metabolism
UDP-glycosyltransferase 76C3		**+3**			B2	Q9FI96	sugar metabolism
Xylose isomerase	**-3**	**-3**			B4	Q9FKK7	sugar metabolism
Carbohydrate-binding protein (ER)	**+10**					PLY63356	sugar binding
EP1-like glycoprotein 4				**+3**	B3	A0A2J6M017	carbohydrate transport
Sucrose permease			**+4**			Q9FE59	sugar transport
Sugar transport protein		**+4**			B2	O04249	sugar transport
Sugar carrier protein C	**-3**				B2	Q41144	trans-membrane transport
Sugar transporter MSSP2			**+4**			Q8LPQ8	trans-membrane transport
α-expansin-8	**+3**				B2	O22874	structural
Acyl-Esterase	**-4**					A0A2J6M0M4	structural
ADF-cofilin-like protein		**+14**				PLY94096	structural
Cellulose synthase A			**+3**			A2Y0X2	structural
DnaJ 11 chaperone protein-like				**-3**	D1	A0A2J6M976	structural

Dynein light chain	**-3**				B5	PLY65182	structural
Expansin-A1	**-3**				B2	Q9C554	structural
Fasciclin-like arabinogalactan protein 12			**-5**	**-3**	B1	A0A2J6M5I9	structural
Formin-like protein			**+4**			Q84ZL0	structural
Glucomannan 4-β-mannosyltransferase 2	**+3**	**+3**			B1	Q9FNI7	structural
Kinesin	**-7**				D2	PLY73801	structural
KIP1-like protein	**-8**					A0A2J6M0M4	structural
Xyloglucan endotransglucosylase			**-4**	**-4**		P35694	structural
Pectin methylesterase 11	**+3**				B2	Q9SIJ9	structural
Pectin methylesterase inhibitor 61		**+3**			B2	Q9FK05	structural
Rho GTPase activation protein		**-5**				PLY90965	structural
Sulfated surface glycoprotein 185			**+3**			P21997	structural
Villin		**-7**				PLY96337	structural
Xyloglucan endotransglucosylase/hydrolase 22	**+3**				B4	Q38857	structural
Xyloglucan endotransglucosylase/hydrolase 25		**+4**			B4	Q38907	structural
7.3 kDa class II heat shock protein	**+3**				D2	O82013	protein metabolism
Aspartic acid proteinase inhibitor		**+283**			P5	A0A2J6JI63	protein metabolism
Aspartic peptidase		**-3**			D1	PLY86033	protein metabolism
Aspartic peptidase			**-4**		P6	A0A2J6LUS2	protein metabolism
Carboxypeptidase Y		**+4**	**+4**		B1	O13849	protein metabolism
Chloroplast 50S ribosomal protein 5			**+4**			P27684	protein metabolism
Cyclophilin-like peptidyl-prolyl isomerase	**-9**				D2	PLY63056	protein metabolism
Cysteine protease		**+56**			B1	A0A2J6JXM3	protein metabolism

E3 ubiquitin-protein ligase	**+4**				B4	Q6R567	protein metabolism
F-box protein, CPR1-like				**-4**	D1	A0A2J6K198	protein metabolism
GPI-anchor transamidase		**-6**				PLY82490	protein metabolism
Isoaspartyl peptidase/L-asparaginase				**-3**		Q8GXG1	protein metabolism
Metacaspase-1			**+3**			Q7XJE6	protein metabolism
Metalloendoproteinase		**-3**			D1	PLY77300	protein metabolism
Neprosin	**-281**					PLY64833	protein metabolism
Prolyl oligopeptidase	**+21**	**+10**			B2	A0A2J6L9H3	protein metabolism
Protein kinase	**-4**				B2	PLY85533	protein metabolism
Protein methyltransferase		**+3**			B2	PLY97876	protein metabolism
RING-type Zinc finger protein	**-3**				B4	PLY73739	protein metabolism
Serine carboxypeptidase		**+4**	**+4**		B4	PLY92695	protein metabolism
Sec1-like protein	**-5**				D2	PLY73377	protein transport
OPT oligopeptide transporter protein		**+9**			P3	PLY91943	protein transport
Dor1-like family		**+3**				PLY67518	protein trafficking
Calcineurin-like phosphoesterase		**+7**			B1	PLY77054	protein-membrane association
6-phosphogluconate dehydratase	**-488**	**-1877**				PLY86887	Ile & Val metabolism
Isovaleryl-CoA dehydrogenase	**-3**				B1	Q9SWG0	Ile & Val metabolism
Proline dehydrogenase	**-5**	**-8**				PLY62544	Pro & Arg metabolism
Carbamoyl-phosphate synthase	**-12**				B2	PLY87126	Arg metabolism
Amino-acid N-acetyltransferase		**+7**			B5	A0A2J6LRI9	Phe metabolism
3-deoxy-7-phosphoheptulonate synthase	**+3**					P29976	Phe, Tyr & Trp metabolism
Chorismate synthase	**+3**				B2	P27793	Phe, Tyr & Trp metabolism

Prephenate dehydratase	**+11**					PLY90159	Phe, Tyr & Trp metabolism
Tryptophan synthase		**-4**				PLY89119	Trp metabolism
Ribose-phosphate pyrophosphokinase		**-7**				PLY87838	Trp & His metabolism
Formiminotransferase		**+4**				PLY67712	His metabolism
Histidinol dehydrogenase	**-5**				B2	PLY90756	His metabolism
Cobalamin-independent methionine synthase	**+4**	**+7**			B1	Q42699	Met metabolism
Homocysteine methyltransferase			**+5**			Q42699	Met metabolism
Methylthioribose phosphate isomerase	**-42**					PLY86711	Met metabolism
Glutamine Dumper	**+6**	**+6**			D1	PLY84188	amino acid (Glu) export
14-3-3 protein	**-34**				P3	PLY80337	signaling
Arabinogalactan protein 10			**+4**			Q9M0S4	signaling
Auxin responsive protein-like	**-3**				B4	PLY91906	signaling
Auxin-induced protein 15A-like protein			**-4**	**-3**	B4	A0A2J6LX65	signaling
Auxin induced protein 15A-like protein	**+4**				B4	PLY91854	signaling
Auxin-responsive protein SAUR19-like				**-7**	B4	A0A2J6LWY8	signaling
Auxin-responsive protein SAUR21	**-3**				B4	Q9FJF9	signaling
Auxin-responsive protein SAUR21-like				**-4**	B4	A0A2J6LX59	signaling
Farnesyltransferase			**+3**			Q38920	signaling
Fasciclin-like arabinogalactan			**+4**			Q66GR0	signaling
Flotillin family protein		**-11**				A0A2J6JLU1	signaling
Hydroxyproline-rich arabinogalactan 31			**+4**			Q9FZA2	signaling
Inositol bisphosphate phosphatase			**+4**			Q42546	signaling
Phosphatidylethanolamine-binding protein		**-6**				PLY70464	signaling
Phosphatidylinositol kinase		**+5**			D2	PLY68809	signaling

Phosphatidylinositol-phospholipase C		**+3**			P3	A0A2J6M2A7	signaling
Phosphoinositide phosphatase		**-3**				PLY86410	signaling
Rapid Alkalinization Factor (RALF)	**+5**	**+4**			B5	PLY95818	signaling
ABC transporter G family				**+4**	P3	XP_023731515	trans-membrane transport
Adenine/guanine permease AZG1				**+3**	B2	A0A2J6KAH8	trans-membrane transport
Al activated malate transporter	**+4**					A0A2J6MED5	trans-membrane transport
Ammonium transporter			**+4**			O04161	trans-membrane transport
Auxin efflux carrier component 2	**+3**				B4	Q9LU77	trans-membrane transport
Auxin transporter	**+4**				B4	Q8L883	trans-membrane transport
Ctr copper transporter	**-4**					A0A2J6KK95	trans-membrane transport
Cyclic nucleotide-gated ion channel			**+3**			O65718	trans-membrane transport
DETOXIFICATION Protein 32			**+3**			F4I4Q3	trans-membrane transport
Potassium ion channel KAT3	**-84**	**+98**	**-4**		B1	PLY62631	trans-membrane transport
Sodium/calcium exchanger protein	**-17**					A0A2J6JR49	trans-membrane transport
Sulfate permease		**+4**				PLY61735	trans-membrane transport
Vacuolar iron transporter			**+3**			Q9M2C0	trans-membrane transport
WAT1-related protein At3g02690		**+3**			B4	Q93V85	trans-membrane transport
WAT1-related protein At5g40240	**-3**				B4	Q9FL08	trans-membrane transport
Xanthine/uracil/vitamin C permease	**-6**	**-6**			P4	PLY67115	trans-membrane transport
Zn transporter	**-7**	**-10**	**+5**			PLY66784	trans-membrane transport
β-1,3-glucanase			**+3**			Q9M069	stress response
Germin		**-7**			D2	A0A2J6LK00	stress response

Glutathione S-transferase	**+8**	**+15**			B2	PLY67369	stress response
Zinc finger stress-associated protein 8-like			**+4**		B2	A0A2J6LY68	stress response
Alcohol dehydrogenase			**-3**			Q8LEB2	stress response (cold, water)
Dehydration-responsive element-binding protein	**+6**	**+4**			B2	Q9FJ93	stress response (cold, water)
Dehydrin	**-5**			**+3**	D1	A0A2J6LA41	stress response (cold, water)
Late embryogenesis abundant protein	**-5**				P3	A0A2J6JP42	stress response (cold, water)
Raffinose synthase			**+4**			Q5VQG4	stress response (cold)
Choline phosphatase			**+3**			Q41142	stress response (salinity)
Mechanosensitive ion channel		**+4**			B4	PLY99544	stress response (mechanical)
D-mannose binding lectin		**+3**			D2	A0A2J6MF85	stress response (biotic)
Gamma-thionin protein family	**+36**					PLY80357	stress response (biotic)
Thaumatin	**-5**					A0A2J6KVT9	stress response (biotic)
Carbonic anhydrase	**-8**	**-15**	**-4**			F4JIK2	C capture
Ribulose bisphosphate carboxylase	**-10**	**-19**			B2	PLY77539	C capture
Chlorophyll a-b binding protein			**+5**			P27489	photosynthesis
Oxygen-evolving enhancer protein			**+4**			P85194	photosynthesis
Photosynthetic reaction protein		**-5**				PLY63935	photosynthesis
Photosystem II protein D1		**-3**			B4	A7Y395	photosynthesis
Chloroplastic magnesium-chelatase			**+5**			B8ANF1	chlorophyll synthesis
Porphobilinogen synthase			**+4**			Q9SFH9	chlorophyll synthesis
Chlorophyllase-2		**+3**			B4	Q9M7I7	chlorophyll degredation
Geranylgeranyl reductase	**+4**					Q9CA67	carotenoid biosynthesis
WEB family protein		**-3**			D1	PLY97322	chloroplast movement
Light-Regulated WD		**+3**			B1	Q9LPV9	photoperiod sensing

Cupredoxin			**+4**			P29602	electron transport
Cytochrome P450-like protein		**+24**			D2	PLY94036	electron transport
Cytochrome P450 CYP72A219			**-3**		B3	H2DH21	electron transport
Cytochrome P450 709B2			**-4**		B3	F4IK45	electron transport
Cytochrome P450 94A2				**+3**	B4	P98188	electron transport
Mavicyanin			**+5**			P80728	electron transport
NADH dehydrogenase			**+3**			Q8RWA7	electron transport
Photosynthetic NDH subunit 1			**+3**		B2	O80634	electron transport
Photosystem II D1 protein				**+3**	D1	PLY88491	electron transport
Pyridine cytochrome reductase	**+20**	**+4**				PLY91291	electron transport
Quinone oxidoreductase			**+3**		B4	P28304	electron transport
Uclacyanin-3			**+5**			Q96316	electron transport
Umecyanin			**+5**			P42849	electron transport
Cupredoxin			**+4**			P29602	electron transport
2-oxoacid dehydrogenases acyltransferase		**+7**				PLY65660	energy
Aconitase	**-246**				B2	PLY88014	energy
Alternative oxidase	**-17**				P3	A0A2J6LNS1	energy
Fe-dependent oxoglutarate dioxygenase	**-7**	**-11**			B1	Q9FXV6	energy
Isocitrate lyase	**-3**	**-3**			B4	P49297	energy
Malate synthase	**-5**					A0A2J6KHZ8	energy
Malic enzyme	**+1137**	**+1451**				PLY97373	energy
Phosphoglycerate kinase			**+4**			Q9LD57	energy
Pyruvate decarboxylase			**+4**			Q9FFT4	energy

2-oxoacid dependent dioxygenase			**+5**			Q9SKK4	oxidation
Aldo/keto reductase		**+5**			B1	A0A2J6MJ46	oxidation
Ascorbate peroxidase	**-8**					PLY69103	oxidation
Glucose-methanol-choline oxidoreductase		**+5**				PLY72830	oxidation
Glycine dehydrogenase			**+4**			Q94B78	oxidation
Nitrite/Sulfite reductase	**-6**					PLY84996	oxidation
Nucleotide-disulphide oxidoreductase	**-17**	**-10**			D2	PLY82910	oxidation
Catalase			**+5**			P45739	peroxidation
Auxin-responsive protein SAUR23-like			**+4**	**+7**	D1	A0A2J6KJR4	regulatory
Auxin-responsive protein SAUR50-like				**+6**	D1	A0A2J6L9H8	regulatory
BED-type Zinc finger protein			**-3**		D2	A0A2J6K2R0	regulatory
Diketo-phosphopentane phosphatase	**-4**	**-9**				A0A2J6LQC7	regulatory
GRF-type zinc finger protein	**+3**				B4	PLY79713	regulatory
Kinesin-like protein		**+3**			D1	PLY91413	regulatory
Nudix hydrolase 20	**-3**				B4	Q8VXZ0	regulatory
Nudix hydrolase 21	**+3**				B4	Q8VY81	regulatory
Trypsin inhibitor protease		**-8**				PLY85894	regulatory
Acidic endochitinase	**+3**				B2	P29024	plant defense
Adenosylhomocysteinase			**+6**			O23255	plant defense
Chitinase			**+3**			Q7Y1Z0	plant defense
Disease resistance protein At3g14460-like			**+61**		D1	A0A2J6LFH9	plant defense
Disease resistance protein – like protein	**+5**				D1	PLY80535	plant defense

LRR receptor-like serine/threonine-protein kinase FLS2			**-3**		B4	A0A2J6LFU1	plant defense
LRR receptor-like serine/threonine protease		**-5**			B4	PLY68176	plant defense
RP-13-like disease resistance protein	**+3**				B2	PLY97856	plant defense
Alcohol dehydrogenase-like		**+3**			B3	Q9FH04	developmental
Cytokinin dehydrogenase 3	**-3**				D2	Q9LTS3	developmental
Cytokinin hydroxylase	**+3**				B3	Q9FF18	developmental
Glutaredoxin-like protein At5g39865-like			**-3**		B4	A0A2J6KF66	developmental
Light-dependent short hypocotyls 4-like	**+3**	**+3**			D1	PLY96215	developmental
Pectin methylesterase			**+3**			O04886	developmental
Pectinesterase inhibitor	**-4**		**+3**			Q9FK05	developmental
Phosphoribosyltransferase		**-7**			B1	PLY87838	developmental
2-methyl-6-phytyl-1,4-hydroquinone methyltransferase	**+3**				B4	P23525	phenylpropanoid pathway
Caffeic acid 3-O-methyltransferase			**+3**			Q43239	phenylpropanoid pathway
Polyphenol oxidase	**+25**					P43309	phenylpropanoid pathway
Phenylalanine ammonia-lyase			**+3**			O04058	phenylpropanoid pathway
Shikimate kinase		**+3**			B1	PLY86265	phenylpropanoid pathway
Abscisic acid 8'-hydroxylase				**-4**		Q9LJK2	phenolic metabolism
Acetyl-CoA-benzylalcohol acetyltransferase			**-4**			O64988	phenolic metabolism
Alcohol acetyltransferase		**+3**				PLY83872	phenolic metabolism
Carotenoid oxygenase	**-5**					PLY66686	phenolic metabolism

Vanillyl-alcohol oxidase		**+9**				PLY67945	phenolic metabolism
Anthocyanidin 3-O-glucosyltransferase 2			**+3**		P3	A0A2J6LF68	flavonoid biosynthesis
Flavonol synthase		**+3**			B3	Q9M547	flavonoid biosynthesis
Kaempferol 3-O-β-D-galactosyltransferase	**+5**	**+3**			P5	Q9SBQ8	flavonoid biosynthesis
Malonyl-Co A: anthocyanin 3-O-glucoside-6'-O-malonyltransferase				**+3**	B3	A0A2J6JQ78	flavonoid biosynthesis
Naringenin-chalcone synthase	**+6**	**+7**		**-4**		P48387	flavonoid biosynthesis
(-)isopiperitenol/(-)carveol dehydrogenase				**+3**	B4	A0A2J6LKE0	terpenoid synthesis
3-hydroxy-3-methylglutaryl-CoA reductase	**+3**				B4	P14891	terpenoid synthesis
3-hydroxy-3-methylglutaryl-CoA reductase		**+3**			B4	P29057	terpenoid synthesis
Diphosphocytidyl-methyl-erythritol kinase			**+3**			P93841	terpenoid synthesis
Germacrene A synthase short form	**-3**				B4	Q8LSC2	terpenoid synthesis
Hydroxy-methylglutaryl-CoA reductase			**+3**			P48020	terpenoid synthesis
Terpene synthase	**+16**	**+30**			B3	PLY99643	terpenoid synthesis
Costunolide synthase			**+3**			F8S1I0	sesquiterpene lactone synthesis
Oxidosqualene cyclase		**+19**				A0A2J6KHJ6	sterol biosynthesis
Squalene monooxygenase			**+3**			O48651	sterol biosynthesis
Secologanin synthase	**+3**	**+3**			B3	Q05047	alkaloid synthesis
Strictosidine synthase		**-5**			P5	A0A2J6JPZ2	alkaloid synthesis
Caffeoylshikimate esterase			**+5**			Q9C942	lignin production

Laccase (diphenol oxidase) 6	**-7**	**-5**			B1	Q9ZPY2	lignin production
Peroxidase 47	**-3**				P6	Q9SZB9	lignin production
Aspartate racemase	**-4**					A0A2J6MED5	stereochemistry
Dirigent protein-like protein	**-4**	**-13**		**-8**	B2	Q9SS03	stereochemistry
Dirigent protein 4	**-3**		**-3**		D1	A0A2J6K9W1	stereochemistry
Dirigent protein 23	**+3**	**+3**			B4	Q84TH6	stereochemistry
Dirigent protein 23-like protein				**-6**	B4	A0A2J6KKV6	stereochemistry
Aquaporin	**-7**			**+8**	P3	Q41951	water transport
Aquaporin PIP1-1		**+3**			B2	P61837	water transport
Aquaporin PIP1-3	**-3**	**+3**			B2	Q08733	water transport
Aquaporin PIP1-6	**-3**				B2	Q9ATN0	water transport
Glutamate 5-kinase	**+7**				B2	PLY91259	nitrogen metabolism
Glutamine amidotransferase		**+3**			B2	A0A2J6LYQ3	nitrogen metabolism
High-affinity nitrate transporter	**-7**					A0A2J6LPZ0	nitrogen metabolism
Nodulin-like protein		**-6**			B1	PLY84544	nitrogen metabolism
BAHD acyltransferase	**-3**				B2	Q9FF86	general metabolism
Carboxylesterase			**+3**			Q9LT10	general metabolism
FMN-dependent α-hydroxy acid dehydrogenase	**-8**					PLY86997	general metabolism
Glyoxalase	**-9**				B1	A0A2J6LXD6	general metabolism

S-adenosyl-L-methionine-dependent methyltransferase	**+4**				D1	PLY80743	general metabolism
Cytolysin	**+6**					A0A2J6M2V0	cell death
Rhodanese like protein		**-8**				A0A2J6LBJ5	senescence
Senescence regulator S40	**-11**				B1	A0A2J6KPX2	senescence
Cellulase	**+3**					A0A2J6L3X4	membrane degradation
DREPP polypeptide		**-8**			B4	PLY83953	membrane synthesis
Mn/Fe superoxide dismutase	**-3**					PLY90327	antioxidant
Peroxiredoxin-2E-1			**+5**			Q69TY4	antioxidant
VIT family protein	**+4**	**+7**				PLY95029	iron transport
Ferritin-3	**+3**				B4	Q948P6	iron regulation
BES1/BZR1 Transcription factor	**+9**		**+4**		B5	PLY76419	transcription
bZIP transcription factor		**-3**			D1	PLY84189	transcription
E2FC Transcription factor	**-3**				P5	Q9FV70	transcription
EN 41Transcription factor	**+3**				B4	Q2HIV9	transcription
EN 42Transcription factor	**+4**				B4	Q700E3	transcription
ERF024 Ethylene-responsive transcription factor				**+3**	B2	A0A2J6LYE8	transcription
ERF098 Ethylene-responsive transcription factor			**-4**		P6	A0A2J6KGI9	transcription
Ethylene-responsive transcription factor		**-3**			B2	Q40476	transcription

Ethylene-responsive transcription factor		**-3**			B2	Q8L9K1	transcription
GATA transcription factor 1			**+3**			P69781	transcription
GRAS Transcription factor	**-20**	**-30**			B2	PLY90803	transcription
K-box Transcription factor		**-51**				PLY86436	transcription
MTERF6 Transcription terminator			**+3**			Q9SZL6	transcription
MYB1R1 Transcription factor			**+3**			Q2V9B0	transcription
MYB15Transcription factor	**-3**	**-4**			B4	Q9LTC4	transcription
Myc-type transcription factor		**+3**			B4	PLY77035	transcription
RLTR1Transcription factor		**+3**			B4	Q7XBH4	transcription
SBP-box type transcription factor	**+3**					A0A2J6K871	transcription
Scarecrow-like protein			**+3**			Q9FYR7	transcription
SRF-type transcription factor	**-4**	**+6**			B1	PLY79523	transcription
SWI3C Transcription regulator			**+3**			Q9XI07	transcription
TCP Transcription factor		**+52**			B1	PLY65615	transcription
TFIID Transcription initiation factor		**+49**			B1	PLY74721	transcription
WRKY transcription factor			**+3**		B2	Q93WU8	transcription
YABBY protein		**+6**			D2	PLY84293	transcription
Zinc-finger protein 6-like protein				**+3**	D1	A0A2J6K6I6	transcription
Zinc finger protein 6-like protein			**+4**		D1	A0A2J6LV52	transcription
Light-Dependent Short Hypocotyls 3-like				**+3**	B4	A0A2J6JQ41	transcription (light dependent)
Elongation factor 2		**+6**	**+7**		D2	Q9ASR1	translation
Elongation factor Ts			**-4**			A8G4D2	translation
Rho termination factor	**-5**					PLY75611	translation
RNA polymerase mediator subunit 4		**+4**			B4	PLY80754	translation
Translation elongation factor EF-1		**+5**			B1	PLY82430	translation

Translation initiation factor 4γ			**+3**		Q10475	translation
Malectin		**+5**			PLY72360	post-translational modification
Aminocyclopropane-carboxylate synthase	**-5**				A0A2J6JS65	ethylene synthesis
Formate--tetrahydrofolate ligase	**-3**			B1	P28723	C1 metabolism
Taurine catabolism dioxygenase	**+5**	**+6**			A0A2J6JTE9	sulfur metabolism
Purple acid phosphatase	**+4**				PLY84579	phosphorus metabolism
Inositol polyphosphate phosphatase	**+8**		**-4**		Q8H0Z6	light response
BYPASS1-related protein		**-4**		B4	PLY76197	plant architecture
Lysine-specific demethylase JMJ30			**+3**		Q8RWR1	flowering
Cupin	**+4**	**+8**		D2	A0A2J6KPM1	seed storage protein
Casparian strip membrane protein	**-5**				A0A2J6JLE0	extracellular diffusion
Exocyst component 84		**+5**		B3	A0A2J6KUY4	import
Cyclic nucleotide- and calmodulin-regulated ion channel 5		**+3**		B1	Q8RWS9	Calcium regulation
Stomagen	**-3**				A0A2J6LWN5	stomatal density
S-adenosylmethionine decarboxylase		**+3**			PLY77611	polyamine synthesis
Pinin-like protein		**+3**		B4	PLY94011	cell-cell adhesion
Thioredoxin H9	**+3**	**+3**		B4	Q9C9Y6	cell-cell communication
Topoisomerase		**+4**		B1	PLY97476	DNA replication
Maturase K		**-3**		B1	PLY86761	RNA processing
ADIPOR1 transmembrane protein			**+4**		B7F9G7	unknown
Major latex protein	**-9**				PLY84050	unknown

Matrixin	**-7**	PLY77300	unknown
TMPIT-like protein	**+4**	A0A2J6MJD7	unknown

+, upregulation in association with discolouration; - , down regulated in association with discolouration; P, pinking discolouration; B, browning discolouration; CE, controlled environment conditions.

Table 3. Selected transcripts grouped by the QTL under which they were located, showing increase (+) or decrease (-) in transcription relative to non-discoloured material, association with pinking or browning discolouration in field and controlled environment produced plants, fold change in transcript levels and predicted pathways.

		Phenotype					
		Field		CE			
QTL	**Predicted protein**	**P**	**B**	**P**	**B**	**UniProt ID**	**Pathway or function**
D1	Glutamine Dumper	**+6**	**+6**			PLY84188	amino acid (Glu) export
	Dehydrin	**-5**			**+3**	A0A2J6LA41	stress response (cold, water)
	Dirigent protein 4	**-3**		**-3**		A0A2J6K9W1	stereochemistry
	bZIP transcription factor		**-3**			PLY84189	transcription
D2	Cytochrome P450-like protein		**+24**			PLY94036	electron transport
	Nucleotide-disulphide oxidoreductase	**-17**	**-10**			PLY82910	oxidation
	Elongation factor 2		**+6**	**+7**		Q9ASR1	translation
	Germin		**-7**			A0A2J6LK00	stress response
	YABBY protein		**+6**			PLY84293	transcription
	Pectate lyase	**-5**		**-3**		PLY64620	sugar metabolism
B1	Potassium ion channel KAT3	**-84**	**+98**	**-4**		PLY62631	trans-membrane transport
	TCP Transcription factor		**+52**			PLY65615	transcription
	TFIID Transcription initiation factor		**+49**			PLY74721	transcription
	NAD dependent epimerase		**-11**			A0A2J6KB13	sugar metabolism
	Laccase (diphenol oxidase) 6	**-7**	**-5**			Q9ZPY2	lignin production

	Cobalamin-independent methionine synthase	**+4**	**+7**			Q42699	Met metabolism
	SRF-type transcription factor	**-4**	**+6**			PLY79523	Transcription
	Aldo/keto reductase		**+5**			A0A2J6MJ46	oxidation
	Translation elongation factor EF-1		**+5**			PLY82430	translation
	α-dioxygenase 1			**-3**		Q9SGH6	fatty acid metabolism
	α-mannosidase		**+3**			Q9LFR0	sugar metabolism
	Glycosyl transferase family 8		**+3**			A0A2J6JG41	sugar metabolism
	Isovaleryl-CoA dehydrogenase	**-3**				Q9SWG0	Ile & Val metabolism
	Shikimate kinase		**+3**			PLY86265	phenylpropanoid pathway
B2	GRAS Transcription factor	**-20**	**-30**			PLY90803	transcription
	Glutathione S-transferase	**+8**	**+15**			PLY67369	stress response
	Dirigent protein-like protein	**-4**	**-13**		**-8**	Q9SS03	stereochemistry
	Carbamoyl-phosphate synthase	**-12**				PLY87126	Arg metabolism
	Exostosin		**+11**			PLY73645	sugar metabolism
	Dehydration-responsive element-binding protein	**+6**	**+4**			Q9FJ93	stress response (cold, water)
	Histidinol dehydrogenase	**-5**				PLY90756	His metabolism
	Sugar transport protein		**+4**			O04249	sugar transport
	UDP-glycosyltransferase 76C3		**+3**			Q9FI96	sugar metabolism
	Sugar carrier protein C	**-3**				Q41144	trans-membrane transport
	Chorismate synthase	**+3**				P27793	Phe, Tyr & Trp metabolism
	ERF024 Ethylene-responsive transcription factor				**+3**	A0A2J6LYE8	transcription
	Ethylene-responsive transcription factor		**-3**			Q40476	transcription

	Ethylene-responsive transcription factor		**-3**			Q8L9K1	transcription
	WRKY transcription factor			**+3**		Q93WU8	transcription
	Adenine/guanine permease AZG1				**+3**	A0A2J6KAH8	trans-membrane transport
	Aquaporin PIP1-1		**+3**			P61837	water transport
	Aquaporin PIP1-3	**-3**	**+3**			Q08733	water transport
	Aquaporin PIP1-6	**-3**				Q9ATN0	water transport
B3	Terpene synthase	**+16**	**+30**			PLY99643	terpenoid synthesis
	Glucan endo-1,3-β-D-glucosidase	**-4**				Q94G86	sugar metabolism
	Secologanin synthase	**+3**	**+3**			Q05047	alkaloid synthesis
	EP1-like glycoprotein 4				**+3**	A0A2J6M017	carbohydrate transport
	Flavonol synthase		**+3**			Q9M547	flavonoid biosynthesis
	Malonyl-Co A: anthocyanin 3-O-glucoside-6'-O-malonyltransferase				**+3**	A0A2J6JQ78	flavonoid biosynthesis
B4	Dirigent protein 23-like protein				**-6**	A0A2J6KKV6	stereochemistry
	MYB15Transcription factor	**-3**	**-4**			Q9LTC4	transcription
	EN 42Transcription factor	**+4**				Q700E3	transcription
	Mechanosensitive ion channel		**+4**			PLY99544	stress response (mechanical)
	Dirigent protein 23	**+3**	**+3**			Q84TH6	stereochemistry
	Xylose isomerase	**-3**	**-3**			Q9FKK7	sugar metabolism
	(-)isopiperitenol/(-)carveol dehydrogenase				**+3**	A0A2J6LKE0	terpenoid synthesis
	2-methyl-6-phytyl-1,4-hydroquinone methyltransferase	**+3**				P23525	phenylpropanoid pathway
	3-hydroxy-3-methylglutaryl-CoA reductase	**+3**				P14891	terpenoid synthesis

	3-hydroxy-3-methylglutaryl-CoA reductase		**+3**			P29057	terpenoid synthesis
	β-galactosidase	**-3**				Q9C6W4	sugar metabolism
	EN 41Transcription factor	**+3**				Q2HIV9	transcription
	Germacrene A synthase short form	**-3**				Q8LSC2	terpenoid synthesis
	Glutathione S-transferase		**+3**			P32110	fatty acid metabolism
	Myc-type transcription factor		**+3**			PLY77035	transcription
	NADH-quinone oxidoreductase		**-3**			PLY87786	phenylpropanoid pathway
	RLTR1Transcription factor		**+3**			Q7XBH4	transcription
B5	3-oxo-5-α-steroid 4-dehydrogenase	**-29**				PLY89462	fatty acid metabolism
	Glycosyl hydrolase family 1		**+19**			PLY77220	sugar metabolism
	α-mannosyltransferase		**+17**			A0A2J6LGJ2	sugar metabolism
	BES1/BZR1 Transcription factor	**+9**		**+4**		PLY76419	transcription
	Amino-acid N-acetyltransferase		**+7**			A0A2J6LRI9	Phe metabolism
P3	Aquaporin	**-7**			**+8**	Q41951	water transport
	Late embryogenesis abundant protein	**-5**				A0A2J6JP42	stress response (cold, water)
	Anthocyanidin 3-O-glucosyltransferase 2			**+3**		A0A2J6LF68	flavonoid biosynthesis
P4	Xanthine/uracil/vitamin C permease	**-6**	**-6**			PLY67115	trans-membrane transport
P5	Glucose/ribitol dehydrogenase	**-6**	**-5**			PLY77463	sugar metabolism
	Kaempferol 3-O-β-D-galactosyltransferase	**+5**	**+3**			Q9SBQ8	flavonoid biosynthesis
	Strictosidine synthase		**-5**			A0A2J6JPZ2	alkaloid synthesis
	E2FC Transcription factor	**-3**				Q9FV70	transcription

P6	ERF098 Ethylene-responsive transcription factor		**-4**	A0A2J6KGI9	transcription
	Peroxidase 47	**-3**		Q9SZB9	lignin production

+, upregulation in association with discolouration; - , down regulated in association with discolouration; D, overall discolouration P, pinking discolouration; B, browning discolouration; CE, controlled environment condition

Differential transcript analyses between lines showing either pinking or browning discolouration and the respective non-discolouring lines at harvest (day 0) were made from RNA samples from the extreme lines grown under CE conditions (Table 2) and subsequently from the identified consistent lines from July- and September- harvested trials from 2016.

Although the majority of differentially expressed transcripts were not shared between the two discolouration types, some commonality was indicated, suggesting the involvement of the same metabolic pathways in both cases (Figure 4).

487 Figure 4

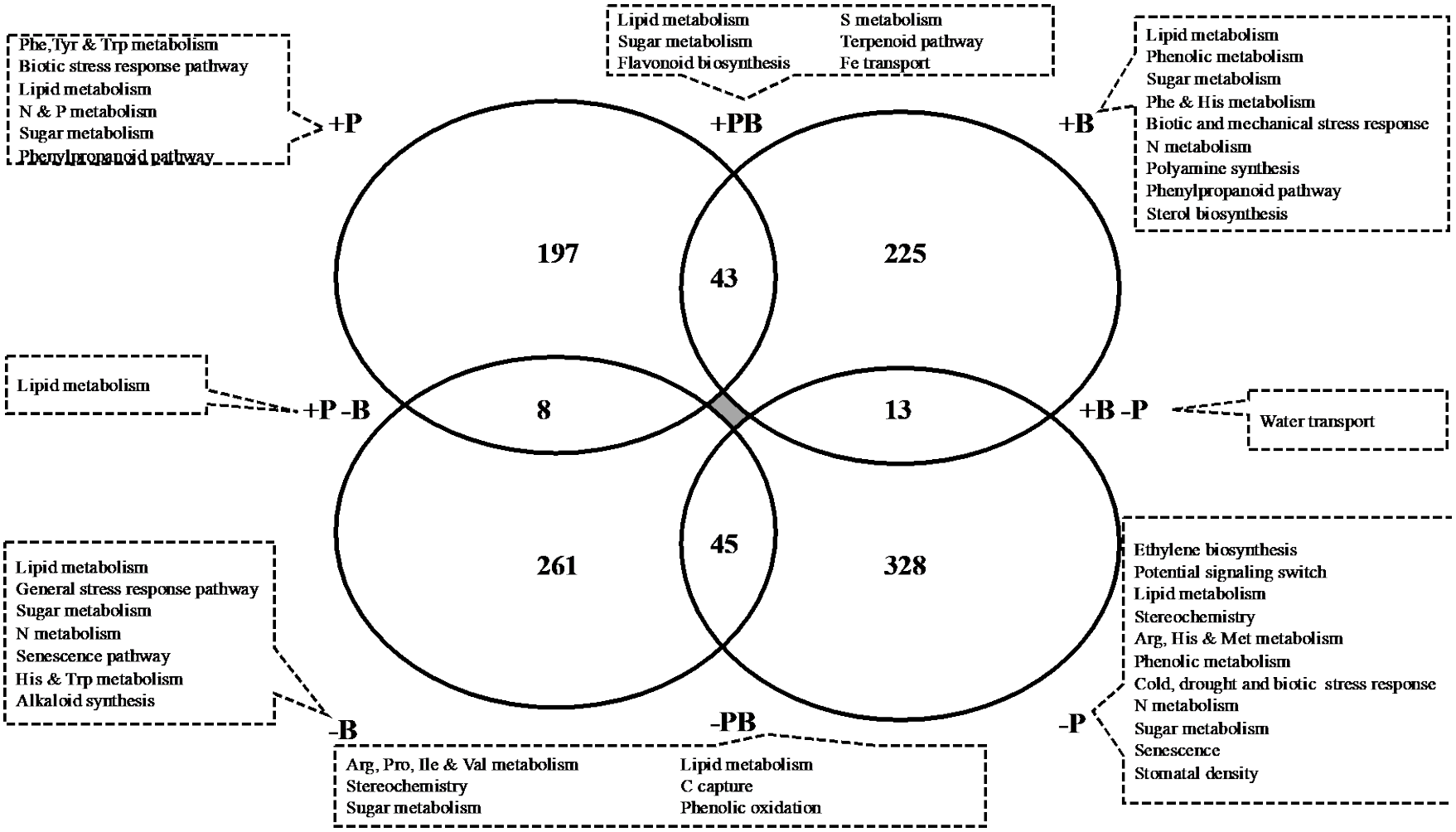

488

Figure 4. Diagrammatic representation of the total numbers of transcripts associated with each different phenotype expression pattern. +P indicates transcripts expressed more highly in pinking, +B indicates transcripts expressed more highly in browning, -P and -B indicate transcripts expressed more strongly in material showing low levels of discolouration (pinking and browning respectively). Categories with only one letter (i.e. P+, rather than P+ B+) indicate transcripts differentially expressed in association with one type of discolouration but not differentially expressed in association with the other, whilst those categories with two letters indicate differential expression associated with both types of discolouration. Call-out boxes indicate typical processes and pathways associated with each category.

3.4 Transcripts located under discolouration QTL

Based on data from the CE trials, primers were designed for qRT-PCR for abscisic acid hydrolase 4, chalcone synthase, PAL and PPO, trans-cinnamate 4-monooxygenase, chalcone-flavonone isomerase, flavonoid-3'-monooxygenase and NAD(P)H-quinone oxidoreductase. qRT-PCR was performed on RNA from field trials 5 and 7 and used to map QTL for all transcripts showing significant variation. QTL for PAL and PPO and NAD(P)H-quinone oxidoreductase co-located with QTL for browning on LG 8a (PAL) and LG 9b (PPO and NAD(P)H-quinone oxidoreductase (Figure 3).

Additional investigation of transcript localization under each of the QTL for discolouration identified a low temperature and drought stress response protein, late embryogenesis abundant protein-like, transcripts associated with the flavonoid and alkaloid pathways, anthocyanidin 3-O-glucosyltransferase (EC 2.4.1.115); kaempferol 3-O-β-D-galactosyltransferase (EC 2.4.1.234) and strictosidine synthase, peroxidase and aquaporin underlying QTL for pinking. A number of transcripts involved in the phenylpropanoid, flavonoid, terpene and alkaloid synthesis, Phe metabolism: chorismate synthase; amino acid N-acetyl transferase, polysaccharide synthesis: glycosyl transferase family 8 and exostosin, a mechanosensitive ion channel, stereochemistry associated functions: dirigent-like proteins and an NAD-dependent epimerase [EC 5.1.3.2], and additional aquaporin genes were found underlying QTL for browning.

Transcripts involved in stress response (e.g. dehydrin) and stereochemistry (dirigent-like proteins) were also located under QTL associated with general discolouration. It is notable that the genomic regions underlying QTL associated with pinking contained a number of genes for which a reduction in transcript expression was associated with browning and *vice versa* (Table 3).

Transcripts for strictosidine synthase showed reduced expression associated with increased browning but was located underneath a QTL for pinking, whilst the gene for Carbamoyl-phosphate synthase (EC 6.3.4.16), showing reduced transcription in association with pinking was located underneath a QTL for browning. This suggests that the pathways resulting in pinking or browning may, in-part, be interrelated, potentially with the same or similar substrates being utilized in different ways.

In addition to enzyme transcripts, a number of transcription factors were identified as being differentially expressed and several of these were detected underlying QTL for pinking and browning. Specifically, BEZ / BRZ type transcription factors were highly expressed in association with pinking, whilst SRF-type transcription factors showed reduced expression in association with pinking and increased expression in association with browning. These two types of transcription factor were found underlying browning QTL 1 and 5, as was a TCP type transcription factor highly expressed in association with browning. Transcription factor types TFIID and YABBY were also found to be highly expressed in association with browning and were found underlying browning QTL 1 and discolouration QTL 2. This would indicate that the transcription level regulation may be important in control of the processes which lead to the development of discolouration, particularly browning.

3.4.1 Transcripts associated with pinking

Transcripts for polyphenol oxidase (PPO) (EC 3.10.3.1) and several enzymes in the phenylpropanoid pathway including phenylalanine ammonia lyase (PAL) (EC 3.4.1.24), the key enzyme responsible for regulating the initial stages of the pathway in plants showed increased expression in plants which subsequently developed high pinking indices compared to those that did not. This was to be expected as PAL activity

has been shown to be induced in response to wounding in plant tissues (Hyodo *et al.,* 1978; López-Galvez *et al.,* 1996; Peiser *et al.,* 1998; Hisaminato *et al.,* 2001), but these transcripts did not show increased expression associated with the development of browning. In addition to PAL and PPO, other transcripts strongly associated with pinking included anthocyanidin 3-O-glucosyltransferase 2, involved in anthocyanin biosynthesis; 3-hydroxy-3-methylglutaryl-CoA reductase (EC 1.1.1.88) and 4-diphosphocytidyl-2-C-methyl-D-erythritol kinase (EC 2.7.1.148) involved in caffeoyl Co-A, isoprenoid biosynthesis; and caffeic acid 3-O-methyltransferase (EC 2.1.1.68) and caffeoylshikimate esterase (EC 3.1.1.-), involved in biosynthesis of caffeic acid derivatives, suggesting the involvement of the phenylpropanoid pathway, specifically caffeic acid.

In addition, transcripts of acetyl-CoA-benzylalcohol acetyltransferase (EC 2.3.1.224) were found to show reduced expression in association with pinking. This enzyme directs carbon away from the phenylpropanoid pathway by converting phenylpyruvate into benzyl acetate instead of phenylalanine. In field-grown material, increased expression of transcripts corresponding to 3-deoxy-7-phosphoheptulonate synthase (EC 2.5.1.54) and prephenate dehydratase (EC 4.2.1.51), which are associated with the assimilation of chorismate into the phenylpropanoid pathway, were also associated with pinking.

Pinking was also associated with increased expression of transcripts for costunolide synthase EC 1.14.14.150), squalene monooxygenase (EC 1.14.14.17), farnesyltransferase (EC 2.5.1.58) and 2-methyl-6-phytyl-1,4-hydroquinone methyltransferase (EC 2.1.1.295), all of which are involved in terpenoid, sequiterpenoid and plant steroid production, and with reduced expression of germacrene A synthase (EC 4.2.3.23) and carotenoid oxygenase (EC 1.13.11.69).

These latter two enzymes are involved in production of sesquiterpenes compounds involved in the development of bitterness and plant defence (Chadwick *et al*., 2013, Chadwick *et al*., 2016) and break-down of carotenoid products of the terpene synthesis pathway respectively. Reduced expression of these transcripts may represent reduced pull-through of resources to these particular endpoints of the terpenoid pathway. Moreover, squalene monooxygenase diverts terpenoid backbone components away from sesquiterpenoid and toward triterpenoid and steroid biosynthetic pathways.

In field-produced material, transcripts encoding sucrose synthase (EC 2.4.1.13), invertase (EC 3.2.1.26) and phosphoenolpyruvate carboxylase kinase (EC 4.1.1.32), involved in the interconversion of sucrose, glucose and fructose showed increased expression in association with pinking, whilst those encoding phosphoglucose isomerase (EC 5.3.1.9), β-galactosidase (EC 3.2.1.23) and glucan endo-1,3-β-D-glucosidase (EC 3.2.1.39), which act on more complex sugars, showed reduced expression. The simple sugars are precursors of the glycolysis cycle which feeds into terpenoid biosynthesis and into the production of non-polar aliphatic amino acids, whilst metabolism of complex sugars would tend to divert resources away from these pathways and is associated with the production of charged aliphatic amino acids in particular arginine. Transcription of enzymes associated with biosynthesis of aromatic amino acids, derived from the shikimate pathway, also showed increased expression in association with pinking.

Saltveit (2018), suggested that the level of pinking observed is dependent on the relative proportion of caffeic acid accumulated in the cells before the action of PPO commences after processing, with higher levels of caffeic acid resulting in more production of caffeoyl-*o*-quinone, which is pink, as opposed to other *o*-diphenols which produce greenish quinones. The overall colour can also be influenced by the amino

601 acids with which *o*-quinones subsequently react and by the levels of antioxidants (AO)
602 which re-convert the *o*-quinones back to their respective *o*-diphenols. The pathways
603 highlighted by the data produced in this study agrees with the Saltveit (2018) model, in
604 that increased transcription of enzymes which promote production of *p*-coumaryl-CoA
605 within the phenylpropanoid pathway should drive the pathway toward production of
606 caffeic acid and thus induce pinking. However, the data we have produced suggests the
607 involvement of at least two other pathways: 1) the flavonoid biosynthesis pathway,
608 which diverts *p*-coumaroyl-CoA away from the production of caffeic acid toward the
609 production of naringenin-chalcone, and 2) the terpenoid biosynthetic pathway, which
610 diverts chorismite, a precursor molecule of the phenylpropanoid pathway, into tyrosine
611 production. According to the model, both of these pathways should reduce pinking as
612 they direct the phenylpropanoid pathway away from caffeic acid production. Our data
613 however shows aspects of both of these pathways associated with the development of
614 both browning and pinking. It is possible that components of these other pathways
615 perform the cycling function of antioxidants (AO) in the Saltveit (2018) model.
616 Damerun *et al.* (2015) have shown that flavanone 3-hydroxylase, involved in the
617 biosynthesis of the flavonoids, is strongly associated with AO activity and that such
618 activity correlated with shelf-life of plant material. However, this was not the case for
619 the carotenoids which were negatively correlated with AO activity. The precise nature
620 of the interaction of these compounds and their impact on discolouration still remains
621 unclear.

622 The other component of the Saltveit model is the amino acids with which the *o*-
623 quinones react. Our data suggests that up-regulation of transcripts in pathways that
624 would likely lead to increased levels of proline, may be associated with the
625 development of pinking. Proline has been associated with expression of stress related

626 genes (Hare *et al.,* 1999, Wang *et al.,* 2015) and in protection against oxidative damage
627 Djabou *et al.* (2017). Accumulation of proline in response to oxidative damage in
628 lettuce may increase availability of proline for interaction with *o*-quinones in the
629 development of pinking. The amino acid tyrosine (Tyr) is synthesized from chorismate
630 and feeds into the biosynthesis of the terpenoid backbone. The direction of chorismate
631 toward the phenylpropanoid pathway would also tend to direct material away from
632 synthesis of Tyr and the terpenoid backbone.

633 As well as diphenols, PPO is able to convert Tyr into dopaquinone. The
634 interaction of quinones with compounds including amino acids is thought to be the
635 source of the discolouration pigmentation in both pinking and browning (Hunter *et al.,*
636 2017; Saltveit, 2018). Hence, enzyme activities which alter the balance of amino acids
637 available for interaction are also likely to influence the final discolouration. In addition
638 to Tyr, genes for enzymes involved in biosynthesis of tryptophan (Trp) i.e. 3-deoxy-7-
639 phosphoheptulonate synthase, chorismate synthase and prephenate dehydratase,
640 showed increased expression in association with pinking, whilst other genes in this
641 pathway (tryptophan synthase and ribose-phosphate pyrophosphokinase [EC 2.7.6.1])
642 showed reduced expression in association with browning.

643 Genes involved in the metabolism of histidine (histidinol dehydrogenase
644 [EC1.1.1.23]) and arginine (carbamoyl-phosphate synthase) were identified as showing
645 reduced expression in association with pinking. The expression of genes for other
646 enzymes involved in the biosynthesis of histidine (ribose-phosphate
647 pyrophosphokinase [reduced expression] and formiminotransferase (EC 2.1.5.2)
648 [increased expression]) were also associated with browning. Both pinking and
649 browning were associated with reduced expression of transcripts for proline
650 dehydrogenase (EC 1.5.5.2); this enzyme converts proline into pyrroline carboxylate,

651 consequently reduced expression of this enzyme would tend to increase available
652 proline for interaction with quinones.
653
654 3.4.2 Transcripts associated with browning
655 Expression of transcripts for shikimate kinase (EC2.7.1.71), which promotes
656 conversion of Trp to chorismite, which subsequently feeds into the phenylpropanoid
657 pathway, was increased in association with browning as were transcripts for amino-acid
658 N-acetyltransferase (EC 2.3.1.36), involved in Phe metabolism. Conversely, transcripts
659 for tryptophan synthase (EC 4.2.1.20) and strictosidine synthase, both of which are
660 involved in the production of alkaloids, a process which directs chorismate away from
661 the phenylpropanoid pathway, showed reduced expression in association with
662 browning.
663 Transcripts representing flavonol synthase (EC 1.14.11.23) and malonyl-Co A:
664 anthocyanin 3-O-glucoside-6'-O-malonyltransferase (EC 2.3.1.171), key components
665 of the flavonoid biosynthesis pathway and specifically anthocyanin production, also
666 showed increased expression in association with browning. Transcripts associated with
667 genes in the carotenoid pathway i.e. abscisic acid 8'-hydroxylase (EC1.14.13.93),
668 associated with the production of phaseic acid, showed reduced expression. This would
669 suggest that the phenylpropanoid pathway is involved with browning as well as pinking
670 although there is an indication that push-through of resources to the flavonoid pathway
671 is favoured in the development of browning.
672 An increase in the biosynthesis of dicaffeoyltartaric, 3,5-dicaffeoylquinic and
673 particularly chlorogenic (5-caffeoylquinic) acids in lettuce has been linked to tissue
674 wounding (Tomás-Barberán *et al.,* 1997; Cantos *et al.,* 2002) and more recently
675 increased levels of 5-*trans*- and 5-*cis*-chlorogenic acids at harvest have been associated

676 with subsequently increased browning in processed Romaine lettuce (García *et al.,*
677 2018, García *et al.,* 2019). The up-regulation of the transcription of genes for shikimate
678 hydroxycinnamoyl transferase (EC 2.3.1.133) (involved in the assimilation and
679 subsequent conversion of *p*-coumaroyl-CoA to caffeoyl-CoA via caffeoylquinic acid)
680 in association with pinking discolouration under CE conditions in this study agrees with
681 these findings. In contrast to García et al., (2018 & 2019), we identified an increase in
682 transcription of caffeic acid *o*-methyltransferase (EC 2.1.1.68), involved in
683 sinapaldehyde synthesis, associated with development of pinking. Garcia *et al*., (2018
684 & 2019) focussed specifically on mid-rib tissue and analysed the biochemistry 5 days
685 post-processing, whilst our study used whole leaf material and investigated pre-existing
686 differences in transcript levels at harvest, subsequently associated with symptom
687 development. Transcript levels, and subsequent expression levels and concomitant
688 biochemistry, may have altered during storage. Moreover, the Garcia studies did not
689 differentiate between pink and brown discolouration, identifying all discolouration as
690 browning (Tomaś-Barberań, 2019, pers. comm.) and was based on Romaine lettuce
691 cultivars (and cultivar-specific differences between metabolite profiles) whilst our
692 work involved a RIL population from a cross between and iceberg and a batavian line.
693 Given the observed negative correlation between pinking and browning and the fact
694 that pinking was not measured by García *et al.* (2018 & 2019) this suggests that
695 increased expression of caffeic acid 3-O-methyltransferase may be associated with
696 reduced browning.

697 Despite the fact that other enzymes directly involved with metabolism of the
698 compounds identified by García *et al.* (2018 & 2019) were not found to be differentially
699 expressed in our work, many of the metabolic pathways indicated are similar;
700 specifically, the phenylpropanoid pathway, which is central to many secondary

metabolic processes in plant cells, the anthocyanin, terpenoid and isoprenoid pathways. We associated up-regulation of transcripts in all of these pathways with increased pinking, and by inference decreased browning, whilst García *et al.* (2019) suggested that these latter three pathways would be responsible for directing carbon flow away from chlorogenic acid production, resulting in decreased browning.

Transcripts associated with the terpenoid pathway that showed increased expression in browning material included 3-hydroxy-3-methylglutaryl-CoA reductase (EC 1.1.1.88), the rate-limiting enzyme in the cytoplasmic melavonate pathway, one of two alternate pathways which leads to terpenoid biosynthesis. The other being the chloroplastic MEP pathway (Lichtenthaler, 1999), (-)isopiperitenol/(-)carveol dehydrogenase (EC 1.1.1.243) and oxidosqualene cyclase (EC 5.4.99.7) which are involved specifically in monoterpene and triterpenoid biosynthesis respectively.

Transcripts for genes involved in complex sugar metabolism, in particular α-mannosidase (EC 3.2.1.24) and α-mannosyltransferase (EC 2.4.x.x) and in polysaccharide production: exostosin, glycosyl transferase families 8 and 61 (EC 2.4.2.x), were increased in association with browning. In addition, an NAD-dependent epimerase, potentially involved with stereochemical interconversion of sugars showed reduced expression. This suggests a role for stereochemical control of the sugar metabolism pathways, particularly complex sugars, in the development of browning. As noted previously, complex sugar metabolism is associated with the production of charged aliphatic amino acids in particular arginine.

In addition to epimerase, other transcripts associated with regulation of stereochemistry, specifically transcripts for a number of dirigent protein-like proteins were also found to show differential expression in association with browning.

Browning was also associated with increased expression of transcripts encoding aquaporin and a potassium- ion channel protein (both which showed reduced expression in association with pinking). These may both be involved in water stress regulation and indicate an environmental influence on the development of browning. Furthermore, browning was associated with increased expression of transcripts for a mechanosensitive ion channel protein which may respond to physical damage.

3.5 Communally expressed transcripts

In field-grown material, increased levels of transcripts associated with metabolism of phenylalanine (Phe), one of the precursors to the phenylpropanoid pathway were associated with both pinking and browning discolouration. Laccase (EC 1.10.3.2) and peroxidase, which are involved in lignin production showed reduced transcription in lines exhibiting pinking or browning compared to respective non-discolouring lines. This would suggest that lignin production is not the endpoint of the pathway(s) leading to these discolourations and that the pathways resulting in either pinking or browning diverge at some point within the phenylpropanoid pathway.

Transcripts encoding naringenin-chalcone synthase (EC 2.3.1.74), an enzyme acting early in the flavonoid pathway converting *p*-coumaroyl-CoA to naringenin-chalcone and terpene synthase (EC 4.2.3.48), which acts in the sesquiterpenoid pathway were also highly transcribed in association with both pinking and browning in the field samples but not in the CE samples, with terpene synthase showing reduced expression in association with browning under CE conditions. Both of these enzymes have been associated with salt and osmotic stress tolerance (Wang *et al.,* 2018, Zhou *et al.,* 2020) in okra and rice respectively, indicating environmental influences on the expression of these genes.

In addition to the three major pathways identified, other functions associated with discolouration include increased expression of genes for the glutamine dumper protein. This protein has been shown to be involved in exudation of glutamine (Glu) from plant hydathodes (Pilot *et al.,* 2004), presumably resulting in a relative increase in the concentrations of other amino acid groups e.g. aromatic amino acids, as well as a non-selective reduction of amino acid concentration in cells and concomitant increase in concentration in the apoplast (Pratelli *et al*., 2020), where they would be available for rapid interaction with quinones released upon processing of the tissue. The release of material from hydathodes is likely to be influenced by water status of the plant, consequently the increased transcription of ion channel proteins, dehydrin and aquaporins observed in browning (and the reduced transcription observed in pinking) may also be associated with this process. Whether greater expression of water transport pore proteins results in increased water uptake or facilitates water loss, however, remains undetermined, however the observation by Monaghan *et al* (2016), that reduced water availability close to harvest has been shown to reduce rib-pinking suggests that reduced transcription of these transcripts may be associated with an overall increase in water status.

A number of other transcripts associated with response to drought stress and low temperature also showed variable expression in pinking, although different transcripts were identified in the CE and field samples. Higher expression of a subset of these genes were associated with pinking in the CE; reduced expression of a different subset was associated with pinking in field samples. This suggests that pinking may be more environmentally susceptible than browning.

Transcripts involved in the stereochemical control of reactions may also have a role to play: Aspartate racemase (EC 5.1.1.13) is responsible for the conversion of L-

775 Asp to D-Asp. L-Asp is involved in the production of coenzyme A (CoA), a key
776 component of the phenylpropanoid pathway. Reduced expression of aspartate racemase
777 (as identified in association with pinking), would suggest that more Asp would be in
778 the L-form and therefore available for conversion into CoA. Dirigent is thought to drive
779 the production of the lignin component (+)-pinoresinol, from the oxidation of two
780 coniferyl alcohol molecules (Davin *et al.,* 1997*).* Whilst the activity of dirigent itself is
781 limited to coniferyl alcohol oxidation (Kim *et al.,* 2002), and lignin production was not
782 associated with discolouration development in this study, other similar proteins could
783 potentially influence the stereochemistry of other oxidative reactions in the
784 phenylpropanoid or related pathways. Given the detection of differential transcription
785 in at least five proteins involved in stereoselection, it is possible that this is a mechanism
786 by which pathways leading to pinking and browning discolouration are differentiated.
787 Most of the pinking-associated transcripts identified as having a role in the
788 phenylpropanoid pathway are downstream of the pathway converting coumaric acid to
789 coumaroyl alcohol. The pathways feeding into or out of this part of the
790 phenylpropanoid pathway would seem to be likely targets for any site of stereoselective
791 activity. Coumaric acid exists in o-, m- and p- isomers, with p-coumaric acid
792 specifically involved in the phenylpropanoid pathway, however o-, and m-coumaric
793 acid have been shown to rapidly inhibit mushroom PPO (Kermasha *et al.,* 1993).
794 Inhibition of PPO is likely to result in reduced pinking and/or increased browning,
795 based on our observation of increased levels of PPO transcription associated
796 specifically with pinking. Furthermore, the immediate precursor of coumaric acid,
797 cinnamic acid exists as both cis- and trans- isomers. The enzyme which catalyses this
798 step, trans-cinnamate-4-monooxygenase (EC 1.14.1491), is trans-isomer specific. Cis-
799 cinnamic acid levels have been shown to be increased by exposure to light, particularly

UV in Arabidopsis (Wong *et al*., 2005). Increased UV would be associated with increased sunlight and therefore temperature, which could result in increased water stress. This in turn could lead to reduced pinking and/or increased browning, according to the data presented in this study.

4 Summary

This work provides novel insight into the biochemical pathways and compounds which influence postharvest discolouration in lettuce and their underlying genetic control. Using a population of F_7 RILs (Saladin x Iceberg) with previously reported variation in the development of pinking and browning discolouration, we have observed that pinking and browning phenotype are generally distinct traits under both genetic and environmental control. The pinking and browning phenotypes observed 3 days postharvest were mapped on a revised Saladin x Iceberg genetic map to 6 QTL associated with pinking, 5 QTL associated with browning and 2 QTL associated with general discolouration.

Involvement of the phenylpropanoid pathway was indicated in the development of both forms of discolouration, with conversion of coumaric acid to coumaryl alcohol appearing to be the boundary step beyond which pinking developed. The association of several transcripts involved in stereoselective processes suggest that stereochemical selection, as a result of differential transcriptional control, may be involved in regulating discolouration. The flavonoid and terpenoid biosynthesis pathways and other biochemistry including amino acid metabolism were also found to be involved (Figure 5). The fact that a number of differences in expression were only observed in the field-grown samples suggest that environmental factors may play a role in regulation of the

824 transcription of some of these genes, and consequently in the development of
825 discolouration.

826 The observed genetic control of variation in pink and brown discolouration in
827 fresh-cut lettuce suggest that it should be possible to breed lettuce cultivars with low
828 levels of pinking and browning and the biochemical pathways identified here highlight
829 potential targets for plant breeders. Finally, the role of growing environment underlines
830 the importance of agronomy in maintain postharvest quality of fresh-cut lettuce.

831 Figure 5

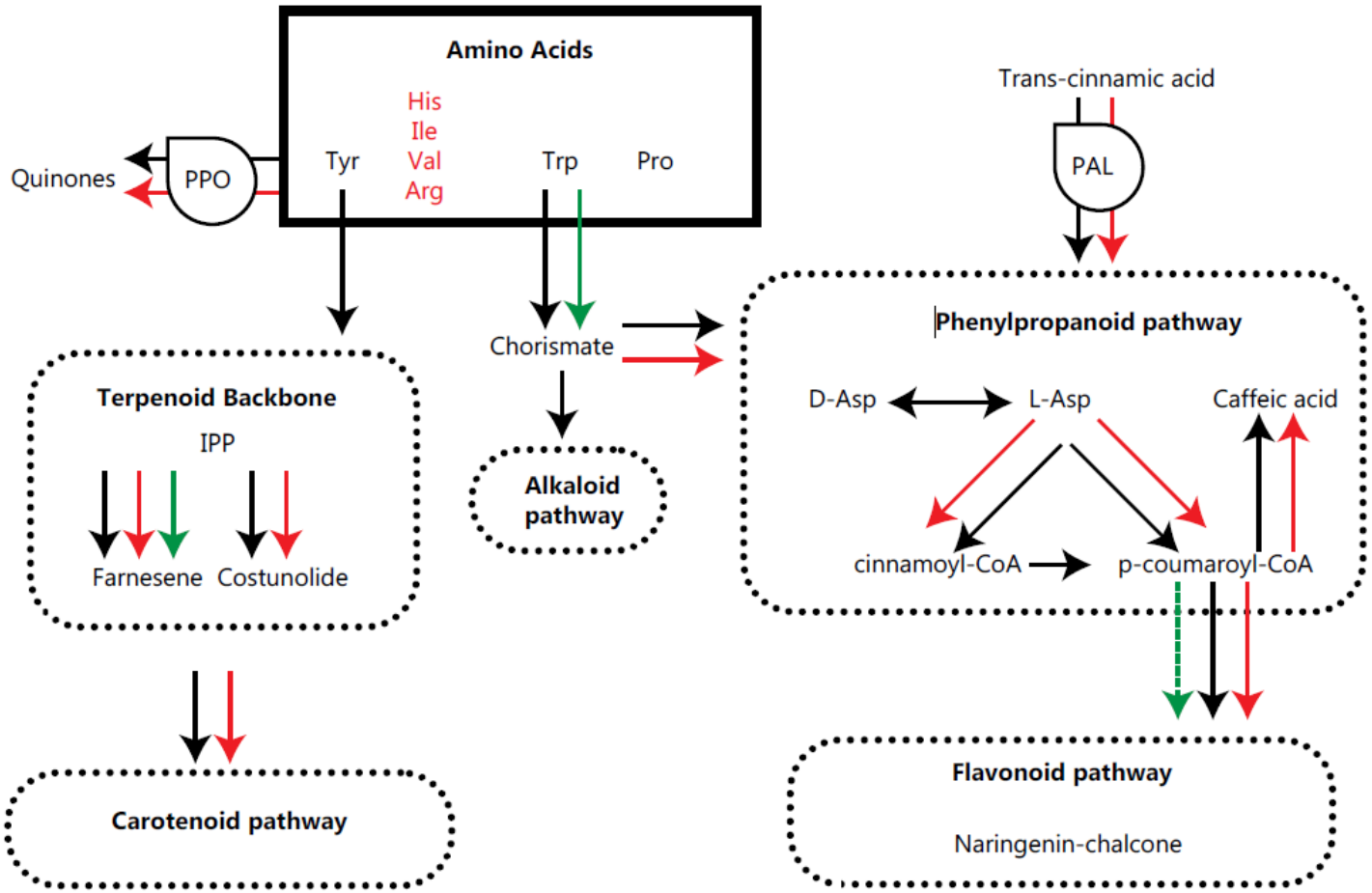

832

Figure 5. Simplified view of the pathways indicated as being involved in pinking and browning development in lettuce based on transcriptome profiles from field-grown and CE-grown material. Simplified pathways are shown in black. Red arrows indicate processes associated with pinking, green arrows indicate processes associated with browning.

5 Acknowledgements

We would like to thank Richard Stark for his invaluable statistical help and Rijk Zwaan, Gs growers, Bakkavor, AHDB, and HIP for their support. This work was funded under BBSRC HAPI (Grant No. BB/M017745/1)

6 References

ADAS. Irrigation Best Practice: A Water Management Toolkit for Field Crop Growers. 2007. Available from http://79.170.40.182/iukdirectory.com/iuk/pdfs/A Water Management Toolkit for Field Crop Growers.pdf. (accessed 1/6/2015).

AHDB. The Nutrient management guide (RB209), https://ahdb.org.uk/nutrient-management-guide-rb209.

Altschul, S.F., Gish, W., Miller, W., Myers, E.W., Lipman, D.J., 1990. Basic local alignment search tool. J. Mol. Biol. 215, 403-410. https://doi.org/10.1016/S0022-2836(05)80360-2

Andrews, S., 2010. FastQC: A quality control tool for high throughput sequence data. Available from http://www.bioinformatics.babraham.ac.uk/projects/fastqc/ (accessed 28 May 2018).

Atkinson, L., Hilton, H.W., Pink, D.A.C., 2013a. A study of variation in the tendency for postharvest discolouration in a lettuce (*Lactuca sativa*) diversity set. Intl. J. Food Sci.Technol. 48, 801–807. https://doi.org/10.1111/ijfs.12030.

Atkinson, L.D., McHale, L.K., Truco, M.J., Hilton, H.W., Lynn, J., Schut, J.W., Mitchelmore, R.W., Hand, P., Pink, D.A.C., 2013b. An intra-specific linkage map of lettuce (*Lactuca sativa*) and genetic analysis of postharvest discolouration traits. Theor. Appl. Genet. 126, 2737–2752. https://doi.org/10.1007/s00122-013-2168-8.

Buchfink, B., Xie, C., Huson, D.H., 2015. Fast and sensitive protein alignment using DIAMOND. Nat. Methods 12, 59-60. https://doi.org/10.1038/nmeth.3176.

Bushnell, B., BBMap. www.sourceforge.net/projects/bbmap/

866 Cantos, J.A., Tudela, M.I., Espín, J.C., 2002. Phenolic compounds and related enzymes
867 are not rate-limiting in browning development of fresh-cut potatoes. J. Agric. Food
868 Chem. 50, 3015–3023. https://doi.org/10.1021/jf0116350.

869 Damerun, A., Selmes, S.L., Biggi, G.F. *et al.,* 2015. Elucidating the genetic basis of
870 antioxidant status in lettuce (*Lactuca sativa*). Hort. Res. 2, 15055.
871 https://doi.org/10.1038/hortres.2015.55.

872 Davin, L.B., Wang, H.B., Crowell, A.L., *et al.,* 1997. Stereoselective bimolecular
873 phenoxy radical coupling by an auxiliary (dirigent) protein without an active
874 center. Science. 275, 362–366. https://doi.org/10.1126/science.275.5298.362.

875 Degl'Innocenti, E., Guidi, L., Paradossi, A., Tognoni, F., 2005. Biochemical study of
876 leaf browning in minimally processed leaves of lettuce (*Lactuca sativa* L. var.
877 Acephala). J. Agric. Food Chem. 53, 9980–9984. https://doi.org/10.1021/jf050927o.

878 Djabou, A.S.M., Carvalho, L.J.C.B., Li, Q.X., Niemenak, N., Chen, S., 2017. Cassava
879 postharvest physiological deterioration: a complex phenomenon involving calcium
880 signaling, reactive oxygen species and programmed cell death. Acta Physiol. Plant.
881 39, 91. https://doi.org/10.1007/s11738-017-2382-0.

882 Dobin, A., Davis, C.A., Schlesinger, F., Drenkow, J., Zaleski, C., Jha, S., Batut, P.,
883 Chaisson, M., Gingeras, T.R., 2013. STAR: ultrafast universal RNA-seq aligner.
884 Bioinformatics 29, 15–21. https://doi.org/10.1093/bioinformatics/bts635.

885 Ewels, P., Magnusson, M., Lundin, S., Käller, M., 2016. MultiQC: summarize analysis
886 results for multiple tools and samples in a single report. Bioinformatics 32, 3047–3048.
887 https://doi.org/10.1093/bioinformatics/btw354.

888 García, C.J., Gil, M.I., Tomás-Barberán, F.A., 2018. LC–MS untargeted metabolomics
889 reveals early biomarkers to predict browning of fresh-cut lettuce. Postharvest Biol.
890 Technol. 146, 9-17. https://doi.org/10.1016/j.postharvbio.2018.07.011.

891 García, C.J., Gil, M.I., Tomás-Barberán, F.A., 2019 Targeted metabolomics analysis
892 and identification of biomarkers for predicting browning of fresh-cut lettuce. J. Agric.
893 Food Chem. 67, 5908-5917. https://doi.org/10.1021/acs.jafc.9b01539.

894 Gawlik-Diziki, U., Złotek, U., Świeca, M., 2008. Characterization of polyphenol
895 oxidase from butter lettuce (*Lactuca sativa* var. capitata L.). Food Chem. 107, 129–
896 135. https://doi.org/10.1016/j.foodchem.2007.07.068.

897 Hare, P.D., Cress, W.A., Staden, J., 1999. Proline synthesis and degradation: a model
898 system for elucidating stress-related signal transduction. J. Exp. Bot. 50, 413-434.
899 https://doi.org/10.1093/jxb/50.333.413.

900 Hayes, R.J., Galeano, C.H., Luo, Y., Antonise, R., Simko, I., 2014. Inheritance of
901 decay of fresh-cut lettuce in a recombinant inbred line population from 'Salinas 88' x
902 'La Brillante'. J. Am. Soc. Hort. Res.139, 388–398.
903 https://doi.org/10.21273/JASHS.139.4.388.

904 Hilton, H.W., Clifford, S.C., Wurr, D.C.E., Burton, K.S., 2009. The influence of
905 agronomic factors on the visual quality of field-grown, minimally-processed lettuce. J.
906 Hort. Sci. Biotechnol. 84, 193–198. https://doi.org/10.1080/14620316.2009.11512503.

907 Hisaminato, H., Murata, M., Homma, S., 2001. Relationship between enzymatic
908 browning and phenylalanine ammonia lyase activity of cut lettuce, and the prevention
909 of browning by inhibitors of polyphenol biosynthesis. Biosci. Biotechnol. Biochem. 65,
910 1016–1021. https://doi.org/10.1271/bbb.65.1016.

911 Huerta-Cepas, J., Forslund, K., Coelho, L.P., Szklarczyk, D., Jensen, L.J., von Merring,
912 C., Bork, P., 2017. Fast genome-wide functional annotation through orthology
913 assignment by eggNOG-mapper. Mol. Biol. Evol. 34, 2115–2122.
914 https://doi.org/10.1093/molbev/msx148.

915 Hunter, P.J., Atkinson, L.D., Vickers, L., Lignou, S., Oruna-Concha, M.J., Pink, D.,
916 Hand, P., Barker, G., Wagstaff, C., Monaghan, J.M., 2017. Oxidative discolouration in
917 whole-head and cut lettuce: Biochemical and environmental influences on a complex
918 phenotype and potential breeding strategies to improve shelf-life. Euphytica 213, 180.
919 https://doi.org/10.1007/s10681-017-1964-7.

920 Hyodo, H., Kuroda, H., Yang, S.F., 1978. Induction of phenylalanine ammonia-lyase
921 and increase in phenolics in lettuce leaves in relation to their development of russet

922 spotting caused by ethylene. Plant Physiol. 62, 31–35.
923 https://doi.org/10.1104/pp.62.1.31.

924 Jones, P., Binns, D., Chang, H.Y. *et al.,* 2014. InterProScan 5: genome-scale protein
925 function classification. Bioinformatics 30 1236–1240.
926 https://doi.org/10.1093/bioinformatics/btu031.

927 Kays, S.J., 1999. Preharvest factors affecting appearance. Postharvest Biol. Technol.
928 15, 233–247. https://doi.org/10.1016/S0925-5214(98)00088-X.

929 Kermasha, S., Goetghebeur, M., Monfette, A., 1993. Studies on inhibition of mushroom
930 polyphenol oxidase using chlorogenic acid as substrate. J. Agric. Food Chem. 41, 526-
931 531. https://doi.org/10.1021/jf4043375.

932 Kim, M.K., Jeon, J-H., Fujita, M., Davin, L.B., Lewis, N.G., 2002. The western red
933 cedar (*Thuja plicata*) 8-8′ DIRIGENT family displays diverse expression patterns and
934 conserved monolignol coupling specificity. Plant Mol. Biol. 49, 199–
935 214. https://doi.org/10.1074/jbc.M112.387423.

936 Koukounaras, A., Siomos, A.S., Gerasopoulos, D., Karamanoli, K., 2016. Genotype,
937 ultraviolet irradiation, and harvesting time interaction effects on secondary metabolites
938 of whole lettuce and browning of fresh-cut product. J. Hort. Sci. Biotechnol. 91, 491–
939 496. https://doi.org/10.1080/14620316.2016.1173526.

940 Langmead, B., Trapnell, C., Pop, M., Salzberg, S.L., 2009. Ultrafast and memory-
941 efficient alignment of short DNA sequences to the human genome. Genome Biol. 10,
942 10: R25. https://doi.org/10.1186/gb-2009-10-3-r25.

943 Lee, S.K., Kader, A.A., 2000. Preharvest and postharvest factors influencing vitamin C
944 content of horticultural crops. Postharvest Biol. Technol. 20, 207–220.
945 https://doi.org/10.1016/S0925-5214(00)00133-2.

946 Li, H., Handsaker, B., Wysoker, A., Fennell, T., Ruan, J., Homer, N., Marth,
947 G., Abecasis, G., Durbin, R., 1000 Genome Project Data Processing Subgroup.,
948 2009. The Sequence Alignment/Map format and SAMtools. Bioinformatics. 25, 2078–
949 2079. 10.1093/bioinformatics/btp352.

950 Liao, Y., Smyth, G.K., Shi, W., 2014. FeatureCounts: an efficient general purpose
951 program for assigning sequence reads to genomic features. Bioinformatics 30, 923–
952 930. https://doi.org/10.1093/bioinformatics/btt656.

953 Lichtenthaler, H.K., 1999. The 1-Deoxy-D-xylulose-5-phosphate pathway of
954 isoprenoid biosynthesis in plants. Ann. Rev. Plant Physiol. Plant Mol. Biol. 50, 47-65.
955 https://doi.org/10.1146/annurev.arplant.50.1.47.

956 López-Galvez, G., Saltveit, M., Cantwell, M., 1996. Wound-induced phenylalanine
957 ammonia-lyase activity: factors affecting its induction and correlation with the quality
958 of minimally processed lettuces. Postharvest Biol. Technol. 9, 223–233.
959 https://doi.org/10.1016/S0925-5214(96)00050-6.

960 Love, M.I., Huber, W., Anders, S., 2014. Moderated estimation of fold change and
961 dispersion for RNA-seq data with DESeq2. Genome Biol. Evol. 15, 550.
962 https://doi.org/10.1186/s13059-014-0550-8.

963 Lyons, E., Freeling, M., 2008. How to usefully compare homologous plant genes and
964 chromosomes as DNA sequences. Plant J. 53, 661–673. https://doi.org/10.1111/j.1365-
965 313X.2007.03326.x.

966 Madeira, F., Park, Y.M., Lee, J. *et al.,* 2019. The EMBL-EBI search and sequence
967 analysis tools APIs in 2019. Nucl. Acids Res. 47, W636–W641.
968 https://doi.org/10.1093/nar/gkz268.

969 Martin, M., 2011. Cutadapt removes adapter sequences from high-throughput
970 sequencing reads. EMBnet.journal. 17, 10–12. https://doi.org/10.14806/ej.17.1.200.

971 Martinez, M.V., Whitaker, J.R., 1995. The biochemistry and control of enzymatic
972 browning. Trends Food Sci. Technol. 6, 195–200. https://doi.org/10.1016/S0924-
973 2244(00)89054-8.

974 Monaghan, J.M., Vickers, L.H., Grove, I.G., Beacham, A.M., 2016. Deficit irrigation
975 reduces postharvest rib pinking in wholehead Iceberg lettuce, but at the expense of head
976 fresh weight. J. Sci. Food Agric.97, 1524-1528. https://doi.org/10.1002/jsfa.7895.

977 Ouzounis, T., Parjikolaei, B.R., Fretté, X., Rosenqvist, E., Ottosen, C-O., 2015. Pre-
978 dawn and high intensity application of supplemental blue light decreases the quantum
979 yield of PSII and enhances the amount of phenolic acids, flavonoids, and pigments in
980 *Lactuca sativa.* Front. Plant Sci. 6, 19. https://doi.org/10.3389/fpls.2015.00019.

981 Peiser, G., López-Gálvez, G., Cantwell, M., Saltveit, M.E., 1998. Phenylalanine
982 ammonia lyase inhibitors control browning of cut lettuce. Postharvest Biol. Technol.
983 14, 171–177. https://doi.org/10.1016/S0925-5214(98)00048-9.

984 Peng, H., Luo, Y., Teng, Z., Zhou, B., Bornhorst, E.R., Fonseca, J.M. and Simko, I.,
985 2021. Phenotypic characterization and inheritance of enzymatic browning on cut
986 surfaces of stems and leaf ribs of romaine lettuce. Postharvest Biol. Technol. 181,
987 p.111653. https://doi.org/10.1016/j.postharvbio.2021.111653

988 Pilot, G., Stransky, H., Bushey, D.F., Pratelli, R., Ludewig, U., Wingate, V.P.,
989 Frommer, W.B., 2004. Overexpression of GLUTAMINE DUMPER1 leads to
990 hypersecretion of glutamine from hydathodes of *Arabidopsis* leaves. Plant Cell 16,
991 1827–1840. https://doi.org/10.1105/tpc.021642.

992 Pratelli, R., Voll, L.M., Horst, R.J., Frommer, W.B., Pilot, G., 2010. Stimulation of
993 nonselective amino acid export by glutamine dumper proteins. Plant Physiol. 152, 762-
994 773. https://doi.org/10.1104/pp.109.151746.

995 Pruitt, K.D., Tatusova, T., Maglott, D.R., 2005. NCBI Reference Sequence (RefSeq): a
996 curated non-redundant sequence database of genomes, transcripts and proteins. Nucl.
997 Acids Res. 33, D501–D504. https://doi.org/10.1093/nar/gki025.

998 Queiroz, C., Lopes, M.L.M., Fialho, E., Valente-Mesquita, L., 2008. Polyphenol
999 oxidase: characteristics and mechanisms of browning control. Food Rev. Intl. 24, 361–
1000 375. https://doi.org/10.1080/87559120802089332.

1001 Quinlan, A.R., Hall, I.M., 2010. BEDTools: a flexible suite of utilities for comparing
1002 genomic features. Bioinformatics. 26, 841–842.
1003 https://doi.org/10.1093/bioinformatics/btq033.

1004 R Core Team. 2018. R: A language and environment for statistical computing. R
1005 Foundation for Statistical Computing, Vienna, Austira. https://www.R-project.org/.

1006 Saltveit, M., 2018. Pinking of lettuce. Postharvest Biol. Technol. 145, 41–52.
1007 https://doi.org/10.1016/j.postharvbio.2018.06.001.

1008 Sgamma, T., Pape, J., Massiah, A., Jackson, S., 2016. Selection of reference genes for
1009 diurnal and developmental time-course real-time PCR expression analyses in lettuce.
1010 Plant Methods 12, 21. https://doi.org/10.1186/s13007-016-0121-y.

1011 Simko, I., Hayes, R.J., Truco, M-J., Michelmore, R.W., Antonise, R., Massoudi, M.,
1012 2018. Molecular markers reliably predict post-harvest deterioration of fresh-cut lettuce
1013 in modified atmosphere packaging. Hort. Res. 5, 21. https://doi.org/10.1038/s41438-
1014 018-0022-5.

1015 Soininen, K., 2009. Salads and salad dressings, UK. Mintel Group Ltd. London, UK.

1016 Solomon, E.I., Sundaram, U.M., Machonkin, T.E., 1996. Multicopper oxidases and
1017 oxygenases. Chem. Rev. 96, 2563–2605. https://doi.org/10.1021/cr950046o.

1018 Tomás-Barberán, F.A., Loaiza-Velarde, J., Bonfanti, A., Saltveit, M.E., 1997. Early
1019 wound- and ethylene-induced changes in phenylpropanoid metabolism in harvested
1020 lettuce. J. Am. Soc. Hort. Sci. 122, 399–404.
1021 https://doi.org/10.21273/JASHS.122.3.399.

1022 Toivonen, P.M.A., Brummell, D.A., 2008. Biochemical bases of appearance and
1023 texture changes in fresh-cut fruit and vegetables. Postharvest Biol. Technol. 48, 1–14.
1024 https://doi.org/10.1016/j.postharvbio.2007.09.004.

1025 Van Ooijen, J.W., 2009. MapQTL 6, Software for the mapping of quantitative trait loci
1026 in experimental populations of diploid species. Kyazma B.V. Wageningen,
1027 Netherlands.

1028 Van Ooijen, J.W., 2018. JoinMap 5, Software for the calculation of genetic linkage
1029 maps in experimental populations of diploid species. Kyazma B.V., Wageningen,
1030 Netherlands.

1031 Wang, F., Ren, G., Li, F., Qi, S., Xu, Y., Wang, B., Yang, Y., Ye, Y., Zhou, Q., Chen,
1032 X., 2018. A chalcone synthase gene *AeCHS* from *Abelmoschus esculentus* regulates

flavonoid accumulation and abiotic stress tolerance in transgenic *Arabidopsis*. Acta Physiol. Plantarum 40, 97. https://doi.org/10.1007/s11738-018-2680-1.

Wang, H., Tang, X., Wang, H., Shao, H-B., 2015. Proline accumulation and metabolism-related genes expression profiles in *Kosteletzkya virginica* seedlings under salt stress. Front. Plant Sci. 29. https://doi.org/10.3389/fpls.2015.00792.

Wong, W.S., Guo, D., Wang, X.L., Yin, X.Q., Xia, B., Li, N., 2005. Study of *cis*-cinnamic acid in *Arabidopsis thaliana*. Plant Physiol. Biochem. 43, 929-937. https://doi.org/10.1016/j.plaphy.2005.08.008.

Young, M.D., Wakefield, M.J., Smyth, G.K., Oshlack, A., 2010. Gene ontology analysis for RNA-seq: accounting for selection bias. Genome Biol. 11, R14. https://doi.org/10.1186/gb-2010-11-2-r14.

Zawistowski, J., Biliaderis, C.G., Eskin, N.A.M., 1991. Polyphenoloxidase. In: Robinson, D.S., Eskin, N.A.M. (Eds.), Oxidative enzymes in foods. London: Elsevier Science, pp217–273.

Zhou, H-C., Shamala, L.F., Yi, X-K., Yan, Z., Wei, S., 2020. Analysis of terpene synthase family genes in *Camellia sinensis* with an emphasis on abiotic stress conditions. Sci. Rep. 10, 933. https://doi.org/10.1038/s41598-020-57805-1.